FISEVIER

Contents lists available at ScienceDirect

Process Safety and Environmental Protection

journal homepage: www.journals.elsevier.com/process-safety-and-environmental-protection





Operationalizing resilience: A deductive fault-driven resilience index for enabling adaptation

Lamis Amer^a, Murat Erkoc^{a,*}, Nurcin Celik^a, Esber Andiroglu^b

- ^a Department of Industrial & Systems Engineering, University of Miami, 1251 Memorial Drive, Coral Gables, FL, USA
- b Department of Civil & Architectural Engineering, University of Miami, 1251 Memorial Drive, Coral Gables, FL, USA

ARTICLE INFO

Keywords:
Resilience metric
Composite index
Leading indicators
Sea-level rise
Adaptation
Decentralized wastewater treatment systems

ABSTRACT

The impact of climate change and the dynamic nature of environmental conditions underscore the critical need to enhance resilience of systems and process safety considerations. The efficacy of such efforts primarily depends on how resilience is measured. Among the myriad efforts to quantify resilience, composite indicators have emerged as promising tools. However, these indicators typically employ statistical methods to derive weights for aggregation and rely on statistical homogeneity among indicators which can limit their scope and fidelity. In this study, we propose an alternative novel resilience index derived from a system's structure and the essential conditions for safe operation during and after disruptions. The proposed measure reflects the systems' ability to resist and respond to failures by addressing possibilities of impact propagation to other infrastructure systems. Moreover, it eliminates the need for weights and allows for compensability among its leading indicators. Using a case study based on the on-site wastewater treatment and disposal systems (OSTDS) in South Florida that faces increasing risks due to rising sea levels, we investigate the validity of the proposed index and perform a comparative analysis with statistically-driven measures. Furthermore, we demonstrate the adaptation of the proposed index for decision making within a generalized optimization framework.

1. Introduction and Background

The exacerbating risks due to climate change have increased interest in integrating resilience into adapting urban and rural infrastructure systems. These systems typically consist of critical utilities that fulfill the communities' basic needs by providing vital services such as supplying food, water, and energy, managing waste, and enabling mobility. Since such systems are usually highly complex and interconnected, their disruption may result in debilitating and cascading ramifications that extend over larger areas (Huang and Ling, 2018). To effectively adapt to and safely operate under the adverse effects of climate change, considerable attention has been given to enhancing the resilience of those infrastructure systems. This has proven to be a nontrivial goal that cannot be achieved without understanding how resilience can be assessed and measured.

Resilience measures can be instrumental in setting thresholds and priorities for adaptation decisions. They guide assessing and monitoring the resilience of systems across time and space, thus, helping communities make adaptation decisions at the right time and with proper scope. In this regard, their integration into decision-making can be direct and

indirect. Indirectly, they can help evaluate and validate adaptation solutions. They are particularly beneficial for running "what-if" analyses to explore and analyze decisions under multiple future climate scenarios. Thus, they guide evaluating potential future impacts, identifying risks and opportunities to enhance systems' resilience, and determining the best courses of action (Molinos-Senante et al., 2012). In a more comprehensive and practical approach, resilience metrics can be directly incorporated into decision models as variables. Through assessing potential resilience gains or losses as a result of a set of actions, these variables can be utilized to form "resilience functions" that can serve as objectives or constraints under a structured decision-making model.

The identification of relevant resilience indicators for a given risk is the first critical step in measuring resilience. Basically, an indicator is a quantitative or a qualitative measure derived from a series of observed facts that can reveal the status of a system in a given instance. When evaluated at regular intervals, an indicator can point out the direction of change across different units and through time. In the context of resilience assessment, resilience indicators are specific and measurable characteristics or properties of a system that can be used to *indicate* its

E-mail address: merkoc@miami.edu (M. Erkoc).

^{*} Corresponding author.

level of resilience. The second critical step in this process is to compile the resilience indicators identified in the previous step into a single composite indicator, which is referred to as the resilience index. For complex infrastructure systems, resilience embodies multi-dimensional facets that might be driven by varying perspectives of diverse stakeholders, which can be subjective and compounded. Integrating resilience indicators that represent these multiple perspectives and factors into a multi-dimensional resilience index has been proposed as an effective approach (Beccari, 2016).

The construction of composite indices poses various challenges that affect their validity, including the selection of underlying factors, their measurement, and the operations used to combine them (National Research Council, 2012). Typically, building a composite index follows a systematic process, including identifying the underlying resilience indicators, scaling them, allocating weights, and aggregating them into a single index. The quality and functionality of the composite index depend on the combination of weighting and aggregation schemes. Usually, weights are determined by statistical methods which rely on statistical homogeneity and correlations among indicators. Such approaches can be limiting in capturing the indicators' actual contribution to the composite index representing the phenomenon under study (Nardo et al., 2005). More importantly, the absence of a proper underlying theory can result in misleading conclusions (OECD, 2008).

With this understanding, we propose a novel resilience index that is: i) derived from leading indicators that are precursors of systems' survivability and safe operation post disruptions, ii) designed to fuse these indicators into a multidimensional composite index, and iii) tailored to support a mathematical functional form that can be employed to construct objectives and constraints in decision-making models. In contrast to the traditional approaches that utilize lagging indicators to characterize the so-called resilience trapezoid ex-post, we propose a resilience index that integrates leading resilience indicators. These indicators can predict potential system failure modes (or survival) ex-ante, based on the system structure and its relationship with the surroundings, therefore integrating the fault-tolerance dimension of resilience (Azadeh et al., 2014). The primary motivation of this alternative approach is to detect early signals of systems' failure and thus guide making the right actions for adaptation.

Accordingly, we identify a set of system-related indicators critical to shaping its resilience and develop a set of axioms to establish the relationships among these indicators using a deductive fault analysis (DFA) approach. These axioms are designed to depict the logical sequence of events that enable systems to survive and operate safely, incorporating both operational and environmental failures into a resilience index. In light of the conceptualization of resilience in seminal works by Holling (1973), Gunderson et al. (1995), and Hollnagel et al. (2006), we adopt the resilience definition that encompasses a system's ability to resist disruption, maintain operations during disruption, and recover to full operational capacity after disruption. This definition has also been adopted by several researchers in recent years (Shandiz et al., 2020; Yarveisy et al., 2020; Pawar et al., 2022), particularly in the fields of process safety and environmental protection. Under this view, we propose a resilience index that can capture the system's ability to operate safely and, at the same time, limit the negative environmental impacts of its processes. We design and propose mechanisms for transforming the identified leading indicators to a normalized scale based on preset indicator-specific thresholds and reference points that indicate conditions for safe system operations. By employing the axioms, we devise an aggregation methodology that does not rely on statistical or participatory techniques. This novel approach allows us to assess the criticality of indicators from the outset, eliminating the need for subjective weighting and the associated subjectivity.

We demonstrate the performance of our proposed approach in the context of the *on-site wastewater treatment and disposal systems* (OSTDS) using a real-life case study from South Florida that faces increasing operational and environmental risks due to rising sea levels. The

contributions of the study presented in this paper include *i*) a novel composite aggregation approach designed for resilience-leading indicators using a deductive fault analysis framework, *ii*) a novel transformation method that accounts for minimum operating requirements for each indicator and the relative importance between the indicators, *iii*) a comparative analysis using statistical models that demonstrates the practicality of the proposed fault-driven approach for measuring resilience, and *iv*) a framework that integrates the proposed resilience index into adaptation decision-making is introduced. Moreover, to the best of our knowledge, this study is the first to provide a method that quantitatively assesses the resilience of OSTDS in the context of sea-level rise. Next, we provide a brief review of the relevant literature, before we discuss the details of the proposed approach.

1.1. Resilience indicators

Various taxonomies are introduced in the literature to review and classify quantitative resilience measures by researchers such as Beccari (2016), Hosseini et al. (2016), Asadzadeh et al. (2017), and Chen et al., 2023. In general, the proposed measures in this context can be grouped under two approaches: performance data-driven and structural data-driven. While the former approach typically employs "lagging indicators", which assess the resilience of systems based on their past performance and observed operational data, the latter approach utilizes "leading indicators", which proactively assess systems' responses to current and future disturbances based on their inherent design and structure. Lagging indicators provide quantitative measures for resilience of a system based on its historical performance, which are also referred to as reactive resilience measures in the literature (Patriarca et al., 2019; Ba-Alawi et al., 2020; Núñez-López et al., 2021). They capture the time-dependent performance measure(s) during a system's degradation and recovery phases post disruptions resulting in a multi-phase curvature known as the resilience trapezoid. When sufficient historical data is available, simulation can generate the resilience trapezoid associated with a system subject to specific threats (Pawar et al., 2022). It can also be predicted based on pre-determined probabilistic damage and fragility curves, loss functions, and recovery curves. Lagging indicators are criticized regarding their use as future predictors of systems' response to incidents (Grabowski et al., 2007; Mengolini and Debarberis, 2008). They may provide limited insight into what constitutes a resilient system as they fail to capture its capacities and dependencies within the system components and between the system and its surrounding environment. Moreover, in many cases, data may not be available to model or predict the shape of the resilience trapezoid. Therefore, structure-based measures are proposed as effective alternatives to assess the resilience of dynamic processes and systems (Penaloza et al., 2020).

As an alternative approach, leading indicators, also known as structure-based indicators, rely on a system's intrinsic characteristics, structure, and spatial relationships with its surroundings. These indicators can act as early warning signals for performance issues and are considered proactive resilience measures (Patriarca et al., 2019). It is important to note that we do not imply that leading indicators cannot be derived from performance-based measures. If periodically collected data is available to monitor a system's well-being and assess its performance resilience in day-to-day operations, performance-based measures can serve that purpose (Hollnagel, 2017). However, they may prove ineffective for evaluating the resilience of systems during large-scale disruptive events when historical data is limited or unavailable. Recent literature has proposed structure-based resilience indicators primarily for network-based infrastructure systems, such as transportation networks (Demirel et al., 2015) and power generation and transmission networks (Panteli and Mancarella, 2015). Amer et al. (2023) provide a comprehensive review of leading indicators proposed in the extant literature for a selected group of critical infrastructure systems in the context of resilience to sea-level rise. Such indicators,

which include connectivity, criticality, and accessibility, are used to evaluate the adaptive capacity of a network in the face of potential disruptions to links and/or nodes (Tachaudomdach et al., 2021). They go beyond capturing solely physical operational parameters and can also incorporate socioeconomic factors related to process safety and environmental impacts. To obtain an overall measure of resilience, the leading indicators need to be systematically aggregated or mapped to a resilience function. This critical task is often accomplished using composite indicators as a medium.

1.2. Composite indicators

Composite indicators have been designed in the context of a diverse range of areas, including socioeconomic status, sustainability, and disaster resilience. The typical process for developing a composite indicator consists of seven main steps: (1) establishing the theoretical framework, (2) data selection, (3) imputation of missing data, (4) multivariate analysis, (5) normalization, (6) weighting and aggregation, and (7) validation for robustness and sensitivity against the established theory (OECD, 2008).

Despite the increased research output on disaster resilience in recent years, the application of composite indicators in this context remains in its infancy (Asadzadeh et al., 2017). The majority of the applications are limited to high-level measures of social and community resilience (Orencio and Fujii, 2013), ecological resilience (Kotzee and Reyers, 2016) and agro-ecosystem resilience (Rao et al., 2019). In many cases, global composite metrics are often deployed to compare regions or countries based on Environmental, Social, and Governance (ESG) outlooks (Global, 2020). Few papers have emerged recently focusing on building composite resilience indicators for engineering systems such as energy systems (Lindén et al., 2021), wastewater management systems (Sun et al., 2020), and transportation infrastructure (Vajjarapu and Verma, 2021).

The quality of the resulting composite indicator usually depends on the methodologies used in normalizing, weighting, and aggregating the individual indicators at different levels and the appropriateness and soundness of the underlying theory and the input data. While the appropriateness of the laid-out approach is subject to the judgment of the modeler and expert opinions, the suitability of the data is often assessed by employing multivariate analysis techniques. Typically, the efficacy of a composite depends on the statistical ability to group multiple indicators into a single proxy, which is often governed by the degree of correlations between the indicators. Higher correlation between the indicators implies fewer statistical dimensions resulting in higher suitability of grouping data to form a composite indicator (Nardo et al., 2005). Although this assumption might be valid for some constructs, we contend that it should not be treated as a compulsory precondition for all composite indicators, especially in the context of the resilience of complex systems.

In essence, building composite metrics is analogous to modeling latent variables in the presence of some observed variables (Otoiu et al., 2021). In these models, the direction of the hypothesized causal relationship between the latent construct and its measurable indicators governs the statistical homogeneity of the data. These causal relationships are either reflective or formative. In a reflective relationship, the latent variable is considered to be the determinant (i.e., the cause) of the observed variables, whereas, in the formative relationship, the latter causes the former. Because reflective indicators map to the same underlying latent variable, they need to have substantial mutual associations (Sanchez, 2013). Unlike reflective indicators, formative indicators do not necessarily measure the same underlying constructs; that is, they do not need to be correlated (Blalock, 1982; Becker et al., 2012). Therefore, assessing the suitability of the data must not be irrespective of the established causation theory. This is a fundamental issue that is often overlooked and mistreated in the literature on the formation of composite indicators (Otoiu et al., 2021).

A critical stage in constructing composite metrics is the normalization of data. Because indicators often reflect different dimensions of the phenomena under study, they are measured on different units or scales. As such, normalization is needed to establish a standard basis for comparison and aggregation. Several normalization methods are introduced in the relevant literature, such as ranking, z-score standardization, Min-Max standardization, distance to a reference subject, scaling to the mean, etc. (OECD, 2008). Although these methods are instrumental and widely utilized, they might fail to meet the composite's objectives when developed primarily for measuring engineering systems' resilience. For engineered systems, we argue that the ideal resilience measure must incorporate the operating requirements to ensure the survivability and safety of a system during and after disruptions. In this context, resilience is not merely an indicator of a system's weaknesses or vulnerabilities, as in the case of risk analysis, but it encompasses the system's capacity to resist and respond effectively. Since minimum operating conditions must be satisfied to maintain the functionality and survivability of a system, they must be the central focus and driver in identifying and normalizing the indicators. The transformation methodology in our proposed metric design explicitly employs this view by accounting for the system's operational requirements and the relativity among the leading indicators representing the properties contributing to the sys-

Another crucial step in developing composite metrics is weighting and aggregating the underlying indicators into a unified index. These techniques critically influence the soundness and validity of the composite metrics. Several weighting and aggregation techniques are reviewed in detail in OECD (2008). Weighting techniques generally rely on either statistical or participatory models to inform weights. Statistical models, such as Factor Analysis (FA), Principal Component Analysis (PCA), and Data Envelopment Analysis (DEA), typically group indicators based on the degree of correlation among them. Whereas participatory models, such as Budget Allocation Processes (BAP), Analytic Hierarchy Processes (AHP), and Conjoint Analysis (CA), rely on stakeholders' and experts' opinions to derive weights. While the former approach is ineffectual when no correlations exist among the indicators, the latter might result in a composite biased by the experts' subjective sentiments. They rely on pair-wise comparisons between indicators, making them computationally expensive with a relatively large number of indicators.

Aggregation techniques following the weighting stage are classified according to how they translate weights. Weights can either represent (i) a trade-off, as in the *compensatory* aggregation methods such as linear and geometric aggregation, or (ii) a measure of importance, as in the *non-compensatory* methods demonstrated by the Multi-criteria analysis (MCA) techniques. In the compensatory methods, the poor performance of one indicator can be compensated for by high performance in some other indicators, resulting in a moderate-to-high performance for the aggregated measure. In contrast, in non-compensatory methods, the impact of each indicator on the composite measure is exclusive (Banihabib et al., 2017). Incorporating compensability relations in the composite metric is a pertinent requisite in modeling the resilience of complex systems. For instance, a system's low ability to resist disruptions can be counterbalanced by its ability to adapt and recover, eventually resulting in moderate-to-high system resilience.

2. Methodology

The proposed resilience index employs formative and compensatory relationships. It is *formative* in the sense that the observed variables are assumed to shape resilience. In this case, correlations among the individual indicators are not required, thus eliminating the need to assess the statistical homogeneity of the data. Moreover, high-performing indicators can balance other underperforming ones; thus, the *compensability* effect is incorporated. The proposed aggregation method maps the logically constructed relationships between the individual indicators into a mathematical baseline function for resilience based on a deductive

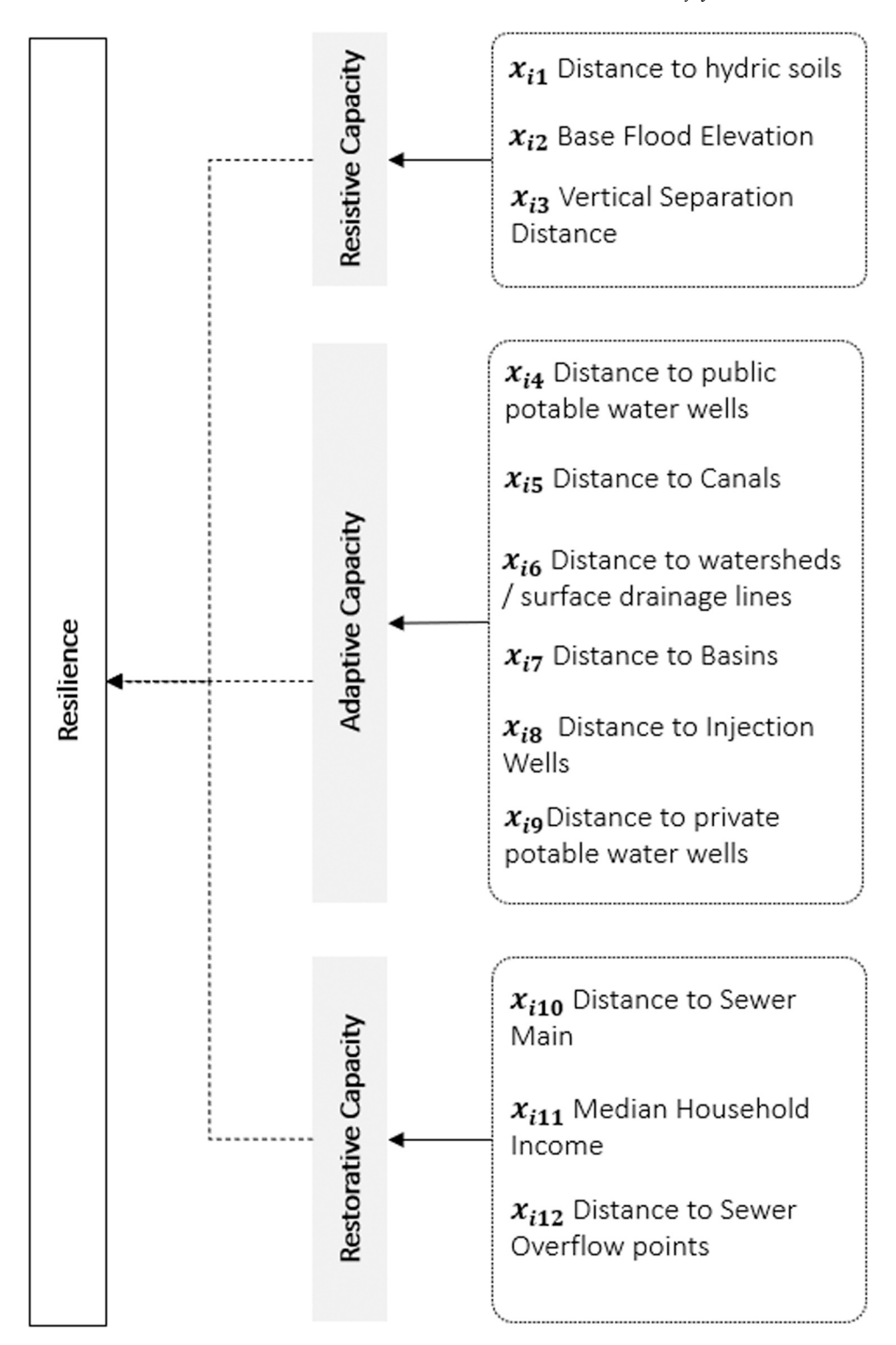


Fig. 1. A hierarchical diagram showing the causal relationships between the identified leading indicators and resilience.

fault-driven analysis. Since the established logical relationships account for the indicators' relative *importance* from the outset, the proposed methodology rules out the need for weighting the individual indicators.

Capturing resilience effectively in this context necessitates a clear understanding of what factors make up a resilient system and how these factors coalesce into the state and functioning of the system. To construct the theoretical foundation and axioms on how the system behaves under current and future sea levels, we start by exploring all direct and indirect relationships between various failure modes

triggered when systems are subject to risks due to sea-level rise. Subsequently, a set of system-related indicators are identified. These indicators are critical in shaping the system's ability to respond, adapt and recover post disruptions. As such, we refer to them as the *resilience-critical* or *resilience leading* indicators. After shortlisting these indicators, we introduce a deductive fault analysis-based methodology for building the composite resilience index. The rationale and mechanisms of the proposed approach are elaborated in the following subsections.

2.1. Theoretical framework

As mentioned earlier, our framework is built in the context of OSTDS, also known as septic systems, that treat and dispose waste from individual properties. In such systems, wastewater is partially treated in the septic tank, where solid waste rests at the bottom of the tank, and the effluent flows from the septic tank to a drain field. The drain field is a set of perforated pipes that discharge effluent to the ground. The discharged waste undergoes final treatment as it percolates through unsaturated soils to the groundwater. For septic systems to function effectively and ensure complete treatment of the effluent before it reaches the groundwater, the soil underneath and surrounding the drain field must be unsaturated, and a minimum vertical separation distance (VSD) between the bottom of the drain field and the high wet season groundwater level must be satisfied. In Florida, the minimum VSD ranges from 12 to 42 in. $(2-4 \text{ ft})(\approx 60-120 \text{ cm})$, depending on the soil percolation characteristics.

With the rising sea levels, septic systems face increasing risks of surface and in-land flooding, both of which may disrupt their proper functioning or cause complete failure. Failed septic systems result in financial burdens to homeowners due to substantial investments in repairs or degraded property values. In addition to their economic impacts, environmental and subsequent public health hazards are of significant concern due to the increased likelihood of contamination of freshwater resources. Contamination occurs when partially treated wastewater containing human-caused Nitrogen (N) mixes with freshwater resources, including groundwater and surface water.

In order to identify the factors shaping the septic system response to sea-level rise risks, we refer to the standards and minimum requirements for safely siting, managing, and operating septic systems as outlined in the EPA 625/1–80–012, Florida Administrative Code (rule chapter 64E-6 +: Standards for OSTDS), and the septic vulnerability report by the Miami-Dade County Department of Regulatory and Economic Resources. We also conducted interviews with officials from the Miami-Dade Water and Sewer Department and the Florida Department of Health, responsible for septic system approval and management. This information was then mapped to a Causal Loop Diagram (CLD) to link various risks (surface flooding and in-land flooding) to septic systems' environmental and hydraulic failure modes (see Appendix A for the CLD

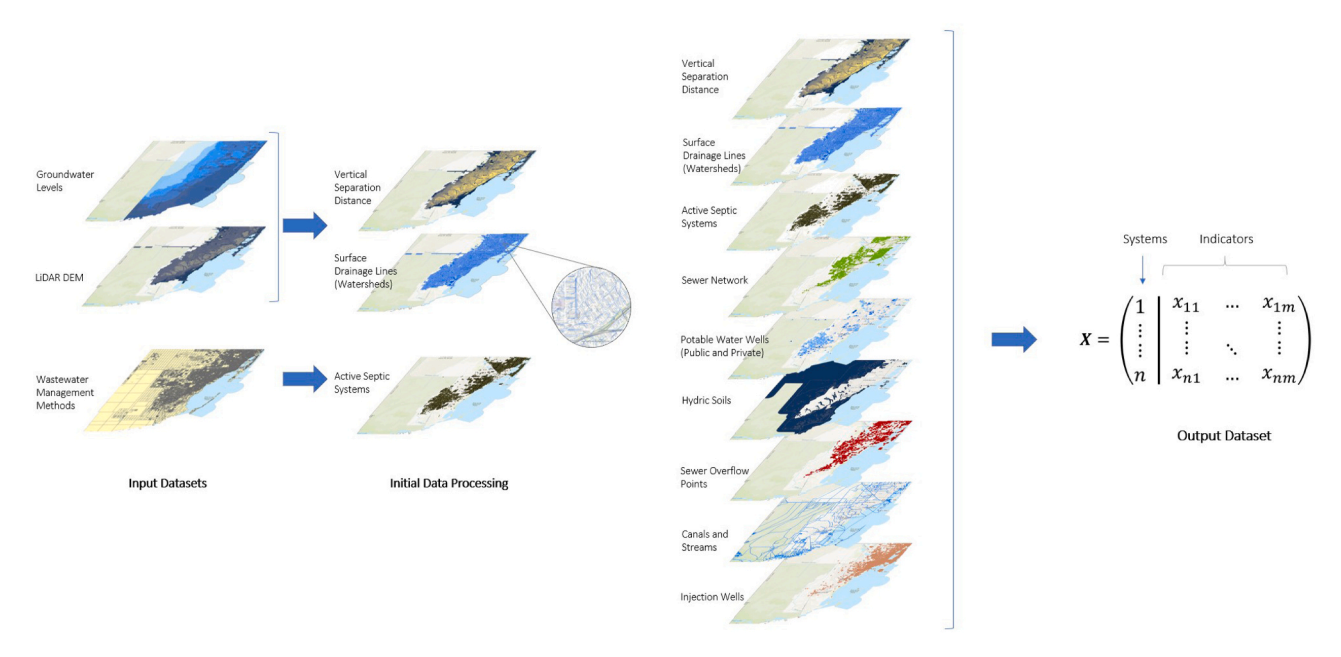
utilized in this study). CLDs visually represent the hypothesized causal relationships between variables or factors in a complex system. Based on this exploratory study, we have identified the root causes of system failure along with other influential factors that contribute to the system's recovery capacity. Overall, we have identified 12 critical indicators that significantly shape the resilience of the OSTDS systems. Since we categorize resilience into three main phases, namely, prevention (resistive or absorption capacity), damage propagation (adaptive capacity), and recovery (restorative capacity), the identified leading indicators are grouped under these categories as listed in Fig. 1 and elaborated in what follows.

2.1.1. Resistive capacity

When exposed to risks, systems with high resistive capacity can withstand failures and sustain their structural and functional integrity. Under sea-level rise, septic systems may experience hydraulic failures due to surface or inland flooding of the drain field. While surface flooding is very likely to occur for systems located within high-risk flood zones, where the base-flood elevation (BFE) is greater than zero, inland flooding may follow rising groundwater levels associated with the rising seas. As the groundwater levels rise above a certain threshold, the vertical separation distance (VSD) is reduced, which may result in inland flooding of the drain field. In addition to hydraulic failures, environmental failures may arise due to a compromised VSD or saturation of soils beneath the drain field caused by excessive precipitation and frequent flooding events. Hence, the distance to hydric soils zones is considered to be a critical factor, along with VSD and Base Flood Elevation (BFE), in determining the system's resistive capacity. The further the site is from an area with hydric soils, the better its ability to resist treatment failures. The factors that influence the resistive capacity of a given septic system i are presented in Fig. 1 and represented by x_{i1} through x_{i3} .

2.1.2. Adaptive capacity

Another component of resilience, the ability of septic systems to adapt to disruptions, is associated with the likelihood and extent of impact propagation to other critical infrastructure systems. This is typically the result of the so-called "domino effect." Domino effect is an undesirable event that emerges in one system and spreads to other



(a) Initial Data Processing

(b) Final Data Processing

Fig. 2. Data Processing

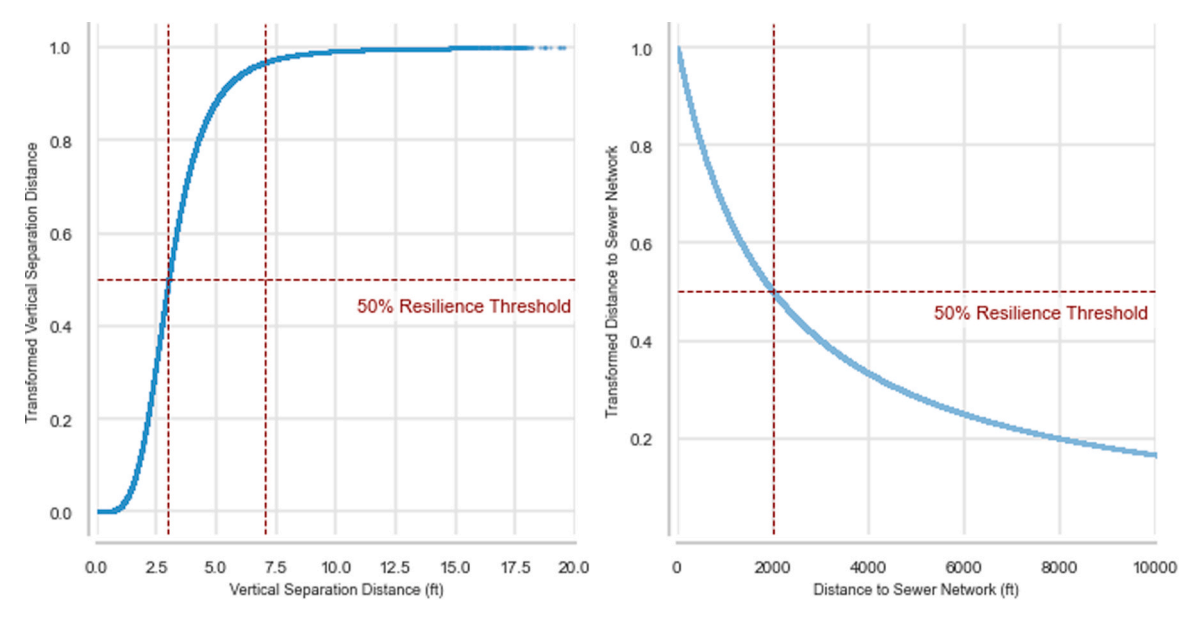


Fig. 3. Transformation curves for the VSD (left) and the distance to sewer lines (right).

systems through escalation vectors. Thus, it causes secondary or highorder events leading to more severe consequences compared to the initial event itself (Tong and Gernay, 2023). In the context of septic systems, a failing system can lead to freshwater contamination through two main streams: i) groundwater contamination and ii) surface water contamination. As discussed earlier, groundwater contamination occurs if the VSD (x_{i3}) is below a minimum threshold or if the soil underneath the drain field is saturated (x_{i1}). In addition, groundwater contamination occurs if a system at risk of surface flooding is proximal to groundwater recharge wells (also known as injection wells) (x_{i8}). These wells are generally utilized to artificially recharge aquifers by surface waters and waters coming from other sources. Surface water contamination is more likely to occur when systems at risk are located in a dense watershed areas, i.e., have dense concentration of surface drainage lines (also known as watersheds) (x_{16}). These surface drainage lines function as transfer channels for the untreated wastewater to nearby surface water bodies, including canals (x_{i5}) and basins (x_{i7}).

Besides the environmental risks, public health risks are expected when potable water resources are contaminated. In this regard, systems close to or within well-field protection zones (x_{i4}) are deemed critical. In the event of groundwater contamination, polluted waters within these zones are more likely to be drawn into potable water wells. Similar relation also applies to proximity to private water wells (x_{i9}) . According to the Florida Department of Health 2020 statistics, nearly 12% of the state population relies on private wells for drinking water consumption. These private wells are not regulated under the federal Safe Drinking Water Act, and as such, the unobserved failures of septic systems close to these private wells pose health risks.

2.1.3. Restorative capacity

In the context of a system's ability to recover, the leading indicators must relate to the technical or socio-economic abilities to recuperate from potential disruptions. On the one hand, the technical factors capture the systems' ability to fully transform into a new state by connecting to alternate wastewater management systems. On the other hand, the socio-economic indicators reflect the household's economic ability to support the recovery of their failed systems. While the former is assessed through proximity to sewer lines (x_{i10}) and existing stresses to the sewer network through observing the sewer overflow locations (x_{i12}), the latter is evaluated based on the median household income (x_{i11}). We consider these indicators to be instrumental in expressing the system's potential for resuming regular wastewater disposal and treatment operations after

a disruption, either by recovering the existing system or transforming its structure.

2.2. Data collection and processing

The input geospatial datasets used in our analysis were obtained from open data sources, including Miami-Dade Open Data Hub, the U.S. Geological Survey (USGS) LiDAR Digital Elevation Model (DEM) at 5 ft ($\approx 1.5 \, \mathrm{m}$) resolution, Groundwater Levels Data at 250 m resolution, and the Wastewater Management Methods embedded in the Florida Water Management Inventory dataset. The input data was processed in two phases, as illustrated in Fig. 2. Three data sets were generated in the initial phase: the vertical separation distance raster layer, surface drainage lines (watersheds) vector layer, and parcels with active septic systems vector data. For septic system (i), given the average ground elevation per parcel (\overline{GL}_i) , the maximum groundwater level (GWL_i^{max}) , and the average standard drain field depth (d), we compute the VSD (xi3) using the following equation:

$$x_{i3} = \overline{GL}_i - d - GWL_i^{max} \tag{1}$$

Watersheds (or surface drainage lines) were generated from the DEM according to the direction of flow accumulating from each grid cell to its steepest down-slope neighbor. Next, data pertaining to parcels with active septic systems was compiled by querying the "wastewater management methods" database for active septic systems. Subsequently, the final data was processed to compute the identified leading indicators for each OSTDS. For this purpose, distances from the center of each parcel with an active OSTDS to the nearest relevant components, such as sewer lines, basins, and potable water wells, were calculated. The resulting data set is an $n \times m$ matrix which we denote by X, where x_{ij} represent the raw value of indicator j for system i, such that $i \in \mathcal{N}$, and $j \in \mathcal{M}$, where $\mathcal{N} = \{1, 2, ...m\}$ is the set of active septic systems, and $\mathcal{M} = \{1, 2, ...m\}$ is the set of indicators.

2.3. Transformation

Since it is often challenging to quantify the absolute value of resilience without any reference or benchmark (Schneiderbauer and Ehrlich, 2006), indicators are typically tailored to assess relative resilience. Relative resilience measures help compare systems and analyze resilience trends over time (Cutter et al., 2008). With this regard, we developed a transformation methodology that standardizes raw

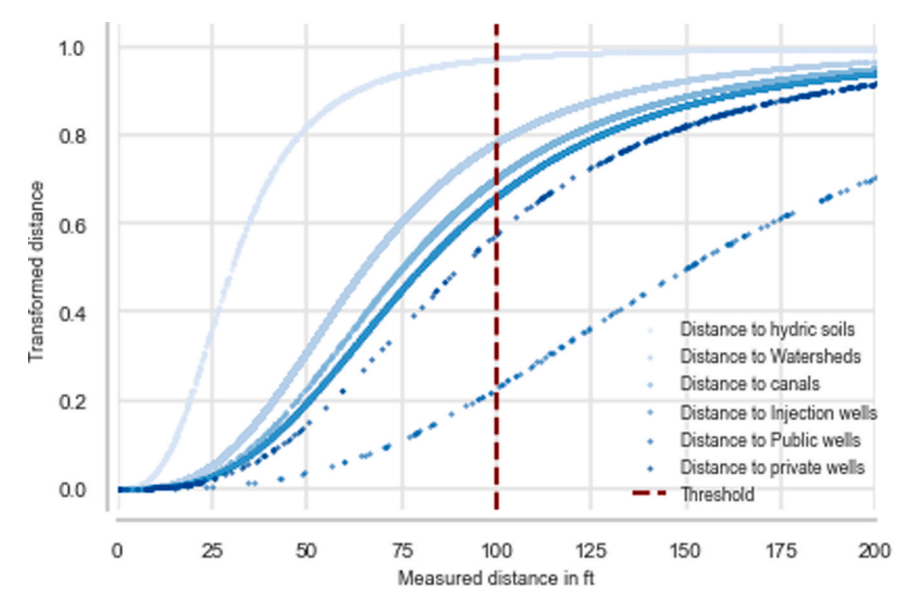


Fig. 4. Transformation curves for several resilient-critical indicators.

indicator values relative to one another to inform and prioritize adaptation decisions. The resilience-critical indicators have positive and negative polarities in the context of the respective system response capacities. In the case of positive polarities, larger values indicate higher resilience. For example, as the VSD at a septic site increases, the system's ability to resist failures caused by inland flooding increases. On the other hand, larger values imply lower resilience for indicators with negative polarities, such as Base Flood Elevation (BFE), where septic systems become more prone to failures resulting from surface flooding as the base flood elevation increases. To account for these positive and negative relations, we employ sigmoid (eq. (2)) and inverse logistic (eq. (3)) transformation functions as given below:

$$x' = \frac{1}{1 + \left(\frac{x_{ij}}{f_j^2}\right)^{-f_j^1}} \tag{2}$$

$$x' = \frac{1}{1 + \left(\frac{x_{ij}}{f_j^2}\right)^{f_j^1}} \tag{3}$$

where x_{ij} denotes the raw value of indicator j for system i, f_j^1 is the parameter to control the shape of the curve, and f_j^2 is the reference value (e.g., 4 ft (≈ 120 cm) for the VSD case). The resulting transformed values range between 0 and 1, where a higher value implies a better ability to respond, hence, a more significant contribution to resilience. Fig. 3 shows the transformation curves for the VSD and the distance to sewer lines as examples.

Reference values and thresholds (f_j^2) signify the "operating variables" that reflect the conditions for safe operation of the system. In a recent study, Pawar et al. (2022) employ a similar approach and map a system's operating variables to resilience indicators. In the context of septic systems, the operating variables are determined based on the recommendations dictated by the OSTDS design, siting, and management manuals published by the U.S. Environmental Protection Agency (EPA 625/1–80–012) and the Florida Administrative Code (rule chapter 64E-6: Standards for OSTDS). In this configuration, values slightly below or almost equal to the minimum threshold (reference value) return a transformed value of 0.5. For instance, the transformation produces a value of 0.5 for a VSD of 4 ft (\approx 120 cm). In the absence of regulated feasible distances, such as distance to sewer lines and sewer overflow, a min-max normalization is performed in the range of [0,1]. An example

of such a case is the distance to sewer lines.

In addition to the minimum operating conditions, the shape parameters (f_j^1) in the transformation functions are tuned to account for the relativity between the indicators. For instance, a septic system located 100 ft (≈ 30 m) from hydric soils is considered more resilient than another system located at an equivalent distance from a potable water wellhead, provided that all other indicators remain the same. Although the system in the former case is close to hydric soils, it still meets the required operating conditions as long as the soil underneath the drain field is suitable for treatment, i.e., the distance to hydric soils is greater than 0. However, for the latter case, the 100 ft distance from potable water wellheads does not meet the minimum required feasible distance, which is 200 ft (≈ 60 m) in Florida. Consequently, the shape parameters for the relevant indicators are selected in a way to satisfy the following ordering:

$$\Gamma_1 > \Gamma_6 > \Gamma_5 \ge \Gamma_7 \ge \Gamma_8 > \Gamma_9 > \Gamma_4,\tag{4}$$

where;

$$\Gamma_{j} = f_{j}^{1} \left[\ln \left(\frac{x_{ij}}{f_{j}^{2}} \right) \right] \quad \forall j \in \mathcal{M} / \{2, 3, 10, 12\}, \forall i \in \mathcal{N}$$

$$(5)$$

The resultant transformation functions are illustrated in Fig. 4. In cases where relative transformations are irrelevant, such as in transforming the VSD, where no other indicators are referenced to this measure, the shape of the transformation function is adjusted to ensure that the transformed value converges to 1 under a zero-risk condition. This is achieved by accounting for the current and expected future sea levels and the associated rise in the groundwater table.

According to the IPCC 6th Assessment Report, under the intermediate greenhouse gas emission scenarios, global sea levels are projected to rise by 0.56 m \pm 0.2 (1.837 ft \pm 0.656) by 2100. In addition, according to USGS and other studies that assess SLR-induced groundwater rise, such as Knott et al. (2019), the projected mean groundwater rise relative to sea-level rise is expected to be 31–35% depending on the distance from the shoreline and other hydraulic characteristics. This means that by 2100, under the worst-case scenario, the rise in the groundwater table will be approximately 0.87 ft (\approx 26 cm). Under this scenario, systems with vertical separation distance nearly greater than or equal to 5 ft (\approx 152 cm) are anticipated to function effectively by 2100, provided that all other conditions are ideal. Based on this inference, the vertical separation distance transformation is adjusted to converge to 1

between 5 and 6 ft (\approx 152–182 cm), as demonstrated in Fig. 3.

2.4. The composite resilience function

We propose a logical aggregation strategy for the indicators founded on failure analysis and systems engineering principles. Systems engineering views systems as complex structures composed of connected multiple elements and modules whose mutual dependencies influence the resultant system reliability. Based on this rationale, we view a septic system as an apparatus whose performance depends on the functionality of multiple other systems or components represented by the leading resilience indicators. These indicators are employed to aggregate a system's resistive capacity (*RC*), adaptive capacity (*AC*), and restorative capacity (*SC*) into a baseline function to define its overall survivability and, thus, resilience based on the hierarchical causal relationship structure illustrated in Fig. 1. These causal relations help us establish a system of axioms that provide the blueprint for the said aggregation. In what follows, we detail these axioms:

Axiom 1. An OSTDS system is said to be highly *resistive* if it can resist both surface and inland flooding. This occurs only if it maintains a high VSD (i.e., large x'), high distance to hydric soils (i.e., large x') and low base-flood elevation (i.e., large x'). If the system fails to achieve at least one of these conditions, it fails to resist disruptions. Mathematically, the system's resistivity is calculated as the product of these factors as represented by the following equation:

$$RC_i = Pr(x' \lor x' \lor x') = \prod_{i=1:3} x'$$
(6)

Axiom 2. A septic system is considered to be *adaptive* if, in the event of failure, impacts can be contained and do not propagate to other infrastructure systems such as drinking water and freshwater resources, groundwater, and surface water. We let IP_{i1} , IP_{i2} , and IP_{i3} represent the likelihood of impact propagation to groundwater, surface water, and drinking water, respectively. Subsequently, the adaptive capacity of septic tank i is abstracted by the following expression:

$$AC_i = 1 - [IP_{i1} \wedge IP_{i2} \wedge IP_{i3}] \tag{7}$$

These Impact propagation components are derived based on the following postulations:

Axiom 2.1. (Groundwater contamination). The likelihood of the septic site impacting groundwater increases as partially treated wastewater seeps into the groundwater resources. One major cause for this is the percolation of partially treated waste through soil due to either proximity to hydric soil *or* compromised VSD. As such, the likelihood of groundwater contamination via soil (GWC_{soils}) is a function of x' and x' and captured by the following equation:

$$GWC_{soils} = 1 - Pr(x' \lor x') = 1 - \left[\prod_{j=1,3} x' \right]$$
 (8)

Another condition causing groundwater contamination is the likelihood of partially treated waste flowing through surface runoff to nearby watersheds or injection wells, which are mapped by x_{i6} and x_{i8} . Consequently, the following function can be used to assess the likelihood of groundwater contamination via surface runoff (GWC_{runoff}):

$$GWC_{Runoff} = 1 - Pr(x' \wedge x') = \left[\prod_{i=6.8} (1 - x') \right]$$
(9)

Subsequently, the impact propagation of septic tank i on ground-water can be computed by the following equation:

$$IP_{i1} = Pr(GWC_{soils} \land GWC_{Runoff})$$

$$= 1 - [(1 - GWC_{soils})(1 - GWC_{Runoff})]$$

$$= 1 - \left[\prod_{j=1,3} x'\right] \left[1 - \prod_{j=6,8} (1 - x')\right]$$
(10)

Axiom 2.2. (Surface Water contamination). The likelihood of the septic site impacting the surface water (IP_{i2}) increases if it gets closer to surface water bodies. Distance to surface water bodies is assessed by the indicators representing proximity to canals (x') and basins (x'). Hence, the impact propagation of septic tank i on surface water can be framed by the following equation:

$$IP_{12} = 1 - Pr(x' \lor x') = 1 - \prod_{i=5,7} x'$$
 (11)

Axiom 2.3. (Drinking Water contamination). The likelihood of the septic site impacting the drinking water resources increases if it gets closer to the water wellheads. Distance to drinking water resources is assessed by the indicators representing proximity to public potable water wells (x') and private potable water wells (x'). In addition, drinking water resources can be indirectly impacted by impact propagation on groundwater. As such, indicators used in Axiom 2.1 are also relevant here. Consequently, the impact propagation of septic tank i on drinking water resources can be modeled by the following equation:

$$IP_{i3} = (IP_{i1}) \left[1 - \prod_{j=4,9} x' \right]$$
 (12)

Given IP_{i1} , IP_{i2} , and IP_{i3} , we can rewrite eq (7) and get the system's ability to adapt to disruptions as follows:

$$AC_i = \prod_{z=1:3} (1 - IP_{iz}) \tag{13}$$

Axiom 3. A system is said to have a high *restorative* capacity if it has the technical *or* the financial abilities to recover or both. The feasibility of sewer extension decisions governs the technical abilities of systems to transfer into a new state and thus recover. This is governed by the pump station basin status, whether it is on moratorium or can accept new connections. On the other hand, the financial ability of communities to recover is guided by the median household income and economies of sewer extensions. This relation can be mathematically abstracted as the following:

$$SC_i = Pr((x' \lor x') \land x') = 1 - (1 - (x' \times x'))(1 - x')$$
 (14)

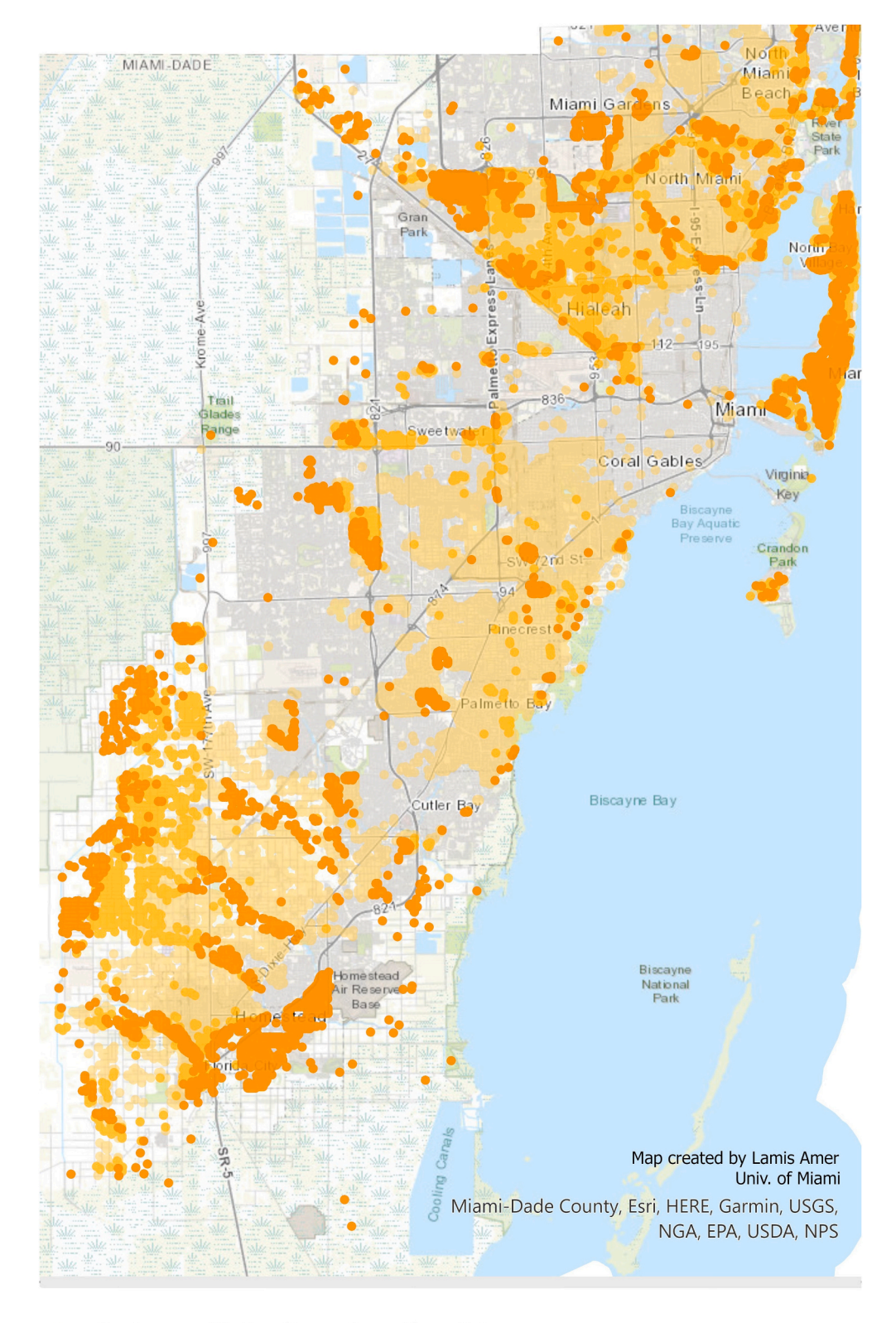
Axiom 4. Finally, a system is said to be *resilient* if it has the ability to resist failure *and* respond to disruptions. The system's overall response capacity is determined by its adaptive *or* restorative capacities or both. Consequently, using equations (6), (13), and (14), we model the overall resilience of a system using the following mathematical expression:

$$R_i = Pr(RC_i \land (AC_i \lor SC_i)) = 1 - [(1 - RC_i)(1 - AC_i \times SC_i)]$$
 (15)

Although this aggregated function is specific to septic systems under study, the presented axioms and the resulting framework can be generalized for applications of other infrastructure systems. An essential requirement is the clear delineation of factors, their impact on the system's failure risk, and how these factors link together to shape the system's overall resilience. In what follows, we demonstrate our approach with application to a real-life septic system network.

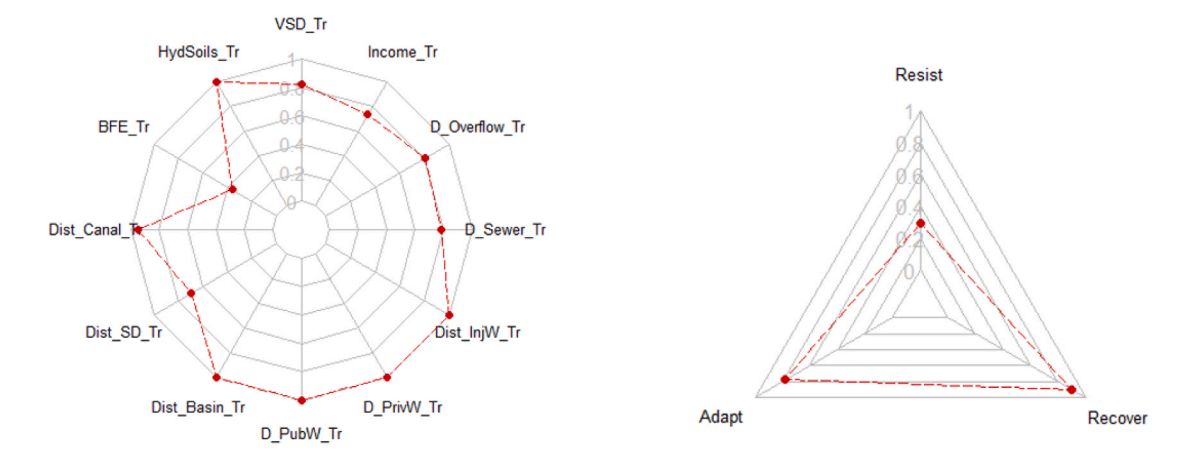
3. Case study

We present a case study concerning the septic systems in Miami-Dade County (MDC) in Florida to demonstrate the application of the proposed

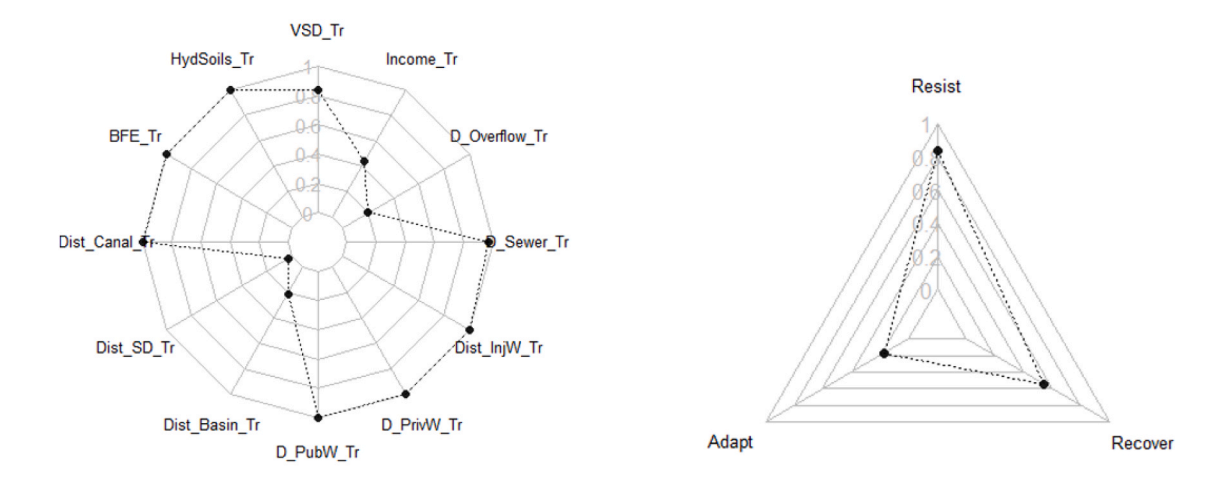


- Systems with Resilience Less than 0.1
- Systems with Resilience Less than 0.5
- Active Septic Systems

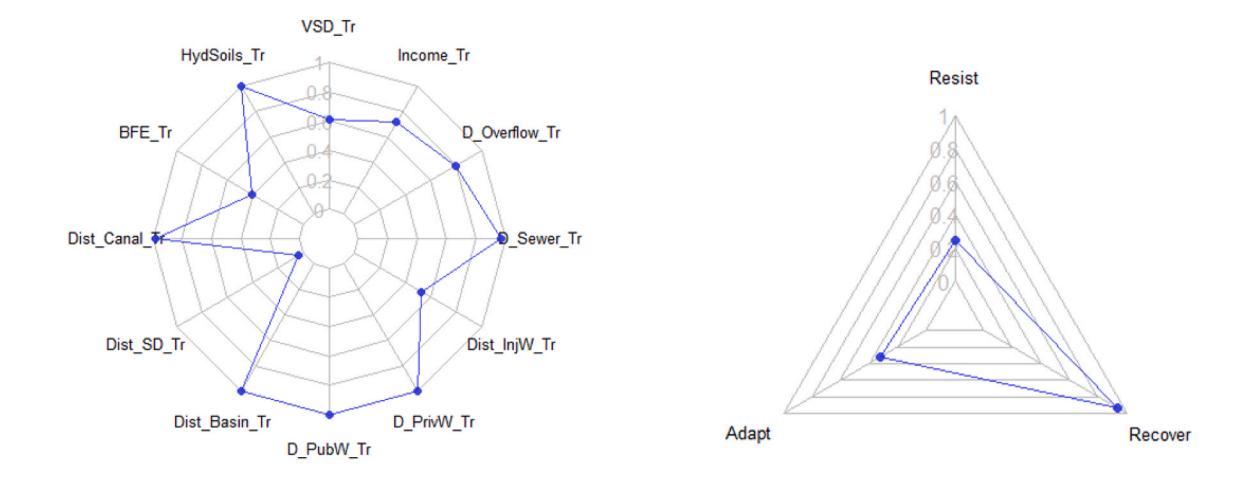
Fig. 5. DFA-based resilience levels for OSTDS in Miami-Dade County, Florida, USA.



(a) System with low resistive capacity but high response capacity (Resilience = 0.79)



(b) System with high resistive capacity but low response capacity (Resilience = 0.86)



(c) System with moderate resistive and response capacities (Resilience = 0.48)

Fig. 6. Baseline resilience measures under varying resistive and responsive capacities.

Table 1The leading indicators and transformed values (distances are given in feet (meters)).

Leading Indicator	Raw Value	Ref. Value	Transformed Value
Vertical Separation Distance (VSD)	3.3 (\approx 1)	$2-4$ (\approx 0.6–1.2)	0.6
Dist to Hydric Soils (HydSoils)	9484.74 (\approx 2890)	75 (\approx 22)	1
Base Flood Elevation (BFE)	7 (\approx 2)	0	0.4
Dist to Surface Drainage (Dist_SD)	21.9 (\approx 6)	50–75 (\approx 15–22)	0.0369
Dist to Basins (Dist_Basin)	37251 (≈ 11354)	75–100 (\approx 22–30)	1
Dist to Canals (Dist_Canal)	300.4 (\approx 91)	75 (\approx 22)	0.98
Dist to Injection Wells (Dist InjW)	82.9 (\approx 25)	75–100 (\approx 22–30)	0.526
Dist to Public Wells (Dist PubW)	10537 ($pprox$ 3211)	100–200 (≈ 30–60)	0.98
Dist to Private Wells (Dist PrivW)	5657.22 (≈ 1724)	75–100 (≈ 22–30)	0.98
Dist to Sewer Lines (Dist_Sewer)	$66.78~(~\approx 20)$	*	0.96
Dist to Overflow (Dist Overflow)	3939.2 (\approx 1200)	*	0.8
Median Household Income (Income)	97500	*	0.7

DFA resilience assessment methodology. Septic systems are commonplace in Florida, where an estimated 2.6 million onsite sewage treatment and disposal systems (OSTDS) serve 30% of the state's residents and visitors. These systems discharge over 426 million gallons of treated effluent daily into the subsurface soil (Lusk et al., 2020). At the county level, according to the Florida Water Management Inventory dataset for parcel-level wastewater management methods, Miami-Dade County has approximately 107,000 active septic systems. In a recent OSTDS vulnerability assessment report, MDC officials reported that, out of these 107,000 septic systems, nearly 56% might be periodically compromised during storms or wet years. With the rising sea levels within the next 25 years, the County expects this number to significantly increase to more than 64% by 2040 (Elmir, 2018).

Using the proposed DFA model, we derive the resilience levels of the 107,526 septic sites located in MDC. The geographical distributions of the sites and their computed resilience values are depicted in Fig. 5. Considering the current sea levels and flood-risk zoning, our assessment indicates that nearly 32% of the existing sites have a resilience index below 0.5, indicating that at least one of the minimum operating requirements is not met for these sites, and around 18% of them have a resilience index less than 0.1. Geographically, Fig. 5 shows clusters of low-moderate resilience sites located in the northern and southern regions of the County. In addition to providing the overall system resilience measures, the DFA framework offers the ability to assess the resilience capacities at sub-aggregate levels, namely, resistive, adaptive, and restorative capacities.

We examine three different septic systems selected from the case study to further illustrate our methodology. These septic sites exemplify three distinct operational and environmental settings and how they impact a system's overall resilience. The first case involves a septic site with low resistive capacity yet high overall resilience. Whereas the second case exemplifies a system with moderate response capacity (low adaptive and high restorative capacities) and high overall resilience. Lastly, we present a system with moderate resistive and response capacities, and overall moderate system resilience. Fig. 6 exhibits how the overall resilience measures for these systems are broken down into their building blocks, namely, the transformed leading indicators, these are: vertical separation distance (VSD_Tr), distance to hydric (saturated) soils (HydSoils_Tr), base flood elevation (BFE_Tr), distance to canals (Dist_Canal_Tr), distance to surface drainage lines (Dist_SD_Tr), distance to basins (Dist_Basin_Tr), distance to public potable water

Table 2Aggregating the transformed indicators into the response capacities and Resilience.

Level	Value
Resist (eq. (6))	0.24
GWC_soils (eq. (8))	0.39
GWC_Runoff (eq. (9))	0.45
IP1 (eq. (10))	0.66
IP2 (eq. (11))	0.01
IP3 (eq. (12))	0
Adapt (eq. (13))	0.32
Recover (eq. (14))	0.93
Resilience (eq. (15))	0.47

well head (D_PubW_Tr), distance to private potable water well head (D_Priv_Tr), distance to injection wells (Dist_InjW_Tr), distance to the nearest sewer line (D_Sewer_Tr), distance to the nearest sewer overflow point (D_Overflow_Tr), and median household income (Income_Tr).

We use the site represented in Fig. 6c as an example to demonstrate the computation process of the composite resilience index. As listed in Table 1, we first identify the measured values of the leading indicators. We normalize these values for the first nine indicators listed in the table using the reference values and the transformation process discussed and illustrated in Section 2.3. Since there are no exogenous reference values for the remaining four indicators, median values are used in obtaining the transformed values in these cases. These transformed values are then plugged into the aggregation functions as detailed in Section 2.4 and the components of the resilience index are obtained as presented in Table 2. Finally, using (15), we compute the resilience index value of 0.48 for this site.

In the first case (Fig. 6a), the base flood elevation is very low (nearly zero), implying a higher likelihood of surface flooding and, therefore, a low ability to resist disruptions. Despite that, since all the other resilience-critical indicators representing the site's response capacity are reasonably high, the system maintains a relatively high resilience level of 0.79. The intuition is that no impacts are anticipated to propagate from this site since the system is not proximal to any drinking water resources or surface water bodies. Moreover, no groundwater contamination is expected due to the relatively large vertical separation distance and unsaturated soil conditions. In the second case (Fig. 6b), a system with low adaptive capacity but high resistive and recovery abilities can still achieve a high overall resilience measure of 0.86. For this system, although impact propagation is a potential risk in the event of failure, the system's high resistivity substantially diminishes the possibility of failure, resulting in a high degree of resilience. In other words, the former capacity is compensated by the latter. Finally, in the third case (Fig. 6c), as expected, the system has a moderate degree of resilience due to its moderate abilities to both resist and respond to disruptions.

These examples demonstrate the effectiveness of the proposed DFA aggregation strategy in aligning with the widely accepted definition of resilience, which accounts not only for risk and vulnerability but also for the system's ability to respond to disruptions through modeling its resistive, adaptive, and restorative capacities. The proposed aggregation method also incorporates the compensatory relationships between the system capacities in the sense that it is possible to observe cases in which a system with low resistance (*resp.* respond) capacity but high response (*resp.* resistance) capacity maintains a moderate-to-high resilience level.

A bivariate statistical analysis is performed to generalize the observations made in the aforementioned example and the relationship between the measured resilience index and the response capacities across all sites. The DFA model output was smoothed using kernel density estimation, as illustrated in Fig. 7, to handle the large dataset and provide a more informative visualization. The analysis indicates that both the resistive and adaptive capacities have a strong positive relationship with the resilience index. The relationship between the restorative

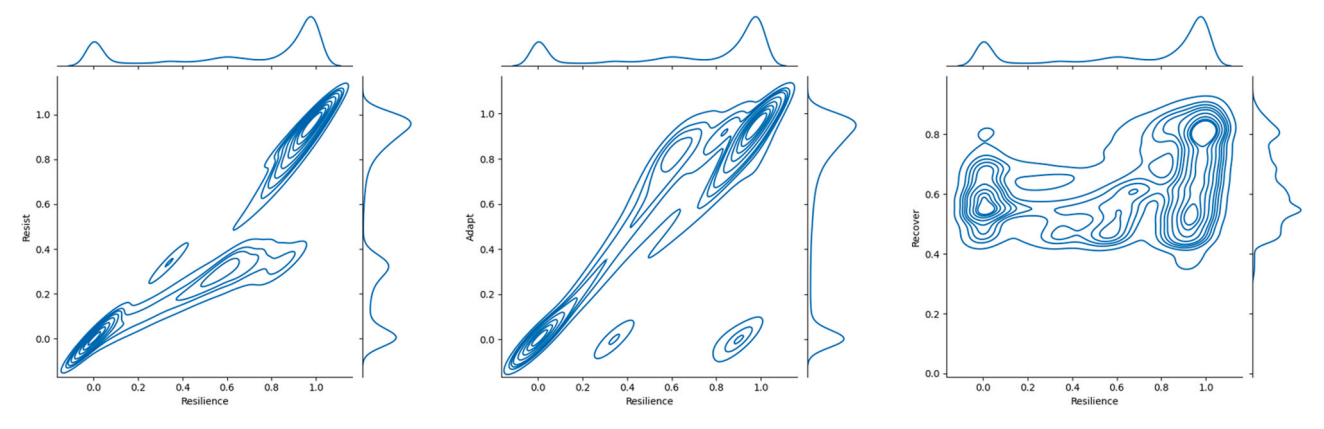


Fig. 7. The relation between resilience and the system's three response capacities.

capacity and overall resilience is more ambiguous. For systems with very poor resistive capacity (less than 0.2), resilience is observed to be strictly low (less than 0.2). Whereas systems with low adaptive capacity (less than 0.2) could possess moderate or high overall resilience. On the contrary, for high resistive and high adaptive capacities, the system's resilience is usually high (greater than 0.8) or moderately high (greater than 0.6), respectively. The computed restorative capacities are generally moderate-to-high (greater than 0.5), with larger values corresponding to slightly higher resilience measures. These observations reflect the compensatory relations between the indicators established by the axioms of the proposed DFA approach.

4. DFA approach vs statistical-driven methods

As detailed in Section 2 and illustrated by the case study in Section 3, the proposed DFA models system resilience as a multidimensional index that explicitly reflects compensability between the associated indicators. To provide a more cogent analysis of the proposed method, we compare the proposed methodology against other statistically-driven models adopted in the context of composite indicators building. The main goal of this discussion is to identify the similarities and gaps between the DFA-based resilience metric and the latter group of models. We aim to derive insights from such a comparison concerning the connotation of resilience implied by different assessment methods. Two statistical models that differ in their weighting strategy are selected for the analysis. The first model is the Partial-Least Squares - Path Model (PLS-PM) for latent variables, which can be viewed as an extension of factor analysis and path analysis. The second model uses Principal Component Analysis (PCA) to derive weights and compute the aggregate scores.

4.1. Partial-least squares path model (PLS-PM)

The variance-based Partial-Least Squares Path Model (PLS-PM) fits a composite model to given data by maximizing the amount of variance explained. Thus, it enables the estimation of complex cause-effect relationships in path models with latent variable(s) that directly or indirectly causes, or is caused by, a group of measured indicators. In this sense, PLS-PM quantifies the hypothesized relations among a hierarchy of manifest (measured) and latent variable(s) using a system of multiple interconnected linear regressions (Sanchez, 2013). Consequently, the model estimates factor loadings representing the correlation between the latent variable(s) and the underlying manifest variables. As such, it provides a measure of the adequacy and significance of the latter in reflecting the latent construct(s) (Kline, 2015). Although the PLS-PM is widely addressed in management, marketing, and psychology (Latan et al., 2017), it has recently been utilized to construct composite indicators, such as in Cataldo et al. (2017), Lauro et al. (2018), and Tomaselli et al. (2021).

Table 3The Measurement Model Loadings.

Measured Indicator	Latent Construct	Loadings
Vertical Separation Distance	Resist	0.41
Distance to hydric Soils		0.25
Base-flood Elevation		0.33
Distance to surface Drainage	IP1	0.06
Distance to injection Wells		0.16
GW Cont = $f(VSD, Soils)$		0.70
Distance to basins	IP2	0.58
Distance to canals		0.42
Distance to public wells	IP3	0.09
Distance to Private Wells		0.15
GW Cont = f(VSD, Soils)		0.76
Distance to sewer lines	Recover	0.36
Distance to sewer overflow		0.35
Median Income		0.29

The PLS-PM tests the theoretically hypothesized causal relationships by developing two sub-models: the measurement model and the structural model. While the measurement model captures the relations between each latent variable and its corresponding measured variables, the structural model formulates the relations among the latent variables. In the context of the axiomatic framework introduced in Section 2.4, the measurement model specifies the relation between the leading resilience indicators and their corresponding latent variables representing the system's response capacities. Because these measurable indicators are perceived as the cause for the latent constructs, formative relations are considered in this analysis. In this case, the latent variables are defined as a linear combination of their corresponding measurable variables. This measurement model is expressed mathematically as follows:

$$\xi_q = \sum_{p=1}^{P_q} \omega_{pq} x_{pq} + \delta_q \quad \forall q \in Q$$
 (16)

where ξ_q is the score of the latent variable (q), x_{pq} are the values for the variables measuring the construct q, ω_{pq} are the coefficients linking each measured variable p to the corresponding latent variable q, and δ_q is the error term representing the fraction of the corresponding latent variable q not accounted by the considered measured variables p. The structural model among the latent variables, on the other hand, is expressed as follows:

$$\xi_j = \beta_{0j} + \sum_{q \in O} \beta_{qj} \xi_q + \delta_j \tag{17}$$

where ξ_j is the generic latent variable, e.g. resilience, β_{qj} is the generic path coefficient interrelating the latent variable q to the generic latent variable j, and ϵ_i is the error term for latent variable j.

We note that an additional intermediate model is needed in our context to map the adaptive capacity constructing blocks, namely IP_1 ,

Table 4The Structural Model Metrics.

Metric	Latent Endogenous Variable	Value
R ² Coefficient of Determination	Adapt	0.96
	Resilience	0.98
Redundancy	Adapt	0.58
	Resilience	0.66
Goodness of Fit Index (GOF)		0.66

Table 5The Structural Model Path Coefficients.

2nd Order Latent	1st Order Latent	Path Coefficient	Significance
Adapt	IP1 (Cont. Groundwater Resources)	0.24	* **
	IP2 (Cont. Surface water resources)	0.31	* **
	IP3 (Cont. Drinking Water Resources)	0.45	* **
Resilience	Resist	0.30	* **
	Adapt	0.36	* **
	Recover	0.34	* **

 IP_2 , and IP_3 as defined in Axiom 2. In that respect, our setting exploits a higher-order PLS-PM model where the parameters are estimated using a two-step approach. In the first step, the first-order latent variables' scores are computed using Principal Component Analysis (PCA). Subsequently, in the second step, the PLS-PM analysis is performed using the computed scores as indicators for the 2nd order constructs, which are adaptive capacity and resilience.

The results for the measurement model are summarized in Table 3. In general, for models assuming formative relations, the loadings of indicators are investigated to determine their absolute contribution to the latent construct. As highlighted in the table, the PLS-PM model identifies the vertical separation distance, the groundwater contamination, and the distance to sewer lines as the primal contributors in shaping the system's resistive, adaptive and restorative capacities, respectively. Since the compromised vertical separation distance is a primal cause of groundwater contamination, the results indicate that the vertical separation distance is pivotal in shaping not only the resistive capacities of the systems but also their adaptive capacities. In this sense, the model's conclusions support the underlying causal theory employed by the proposed DFA approach.

The structural model is applied by analyzing the determination coefficients \mathbb{R}^2 and the redundancy index. In addition, path coefficients' significance level (t-test) and magnitude are also assessed. Results are summarized in Table 4. In this case, endogenous latent variables represent adaptive capacity as defined in (13) and resilience as defined in (15). While the former is shaped by the three impact propagation latent constructs, namely, \mathbb{IP}_1 , \mathbb{IP}_2 , and \mathbb{IP}_3 , the latter is determined by the latent resistive, adaptive, and restorative constructs. \mathbb{R}^2 values of 0.96 and 0.98 for the adaptive and resilience constructs evince the significance of the proposed hierarchical structure in mapping the resilience-critical indicators to the system's response capacities and overall resilience.

The Redundancy Index measures the performance of predicting the structural model given the measurement model. As shown in Table 4, redundancies of 0.58 and 0.66 are obtained for the adaptive capacity and resilience, respectively. These results imply that the resilience construct's adaptive, resistive, and restorative capacities can predict 66% of variability within the resilience indicators. According to research, these values indicate a satisfactory level of explanation in the context of the PLS-PM model (Sanchez, 2013).

Path Coefficients capture the causal relations between variables, specifically the direct effect of a variable in causing another variable. In

Table 6Results of the Principal Component Analysis.

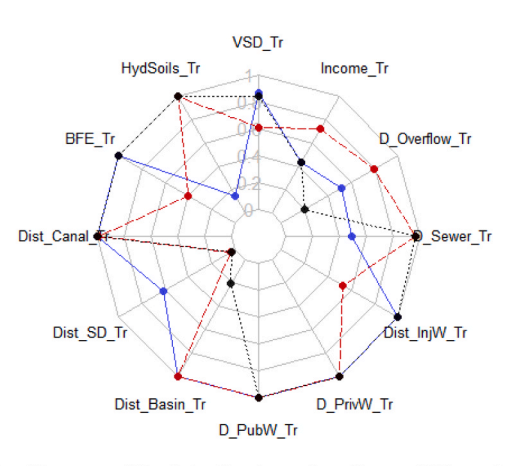
PCA- Stage	Proxies (Latent Vars)	Indicators	Loadings	% Variance
Stage 1	Resist	Base-Flood Elev.	0.31	91.99%
		Vertical Sep. Dist.	0.31	
		Dist. to Hydric Soils	0.37	
	Adapt	GW Cont = $f(VSD, Soils)$	0.11	94.34%
		Dist. to Injection Wells	0.16	
		Dist. to Watersheds	0.07	
		Dist. to Canals	0.16	
		Dist. to Basins	0.16	
		Dist. to Public Wells	0.17	
		Dist. to Private Wells	0.17	
	Recover	Dist. to Sewer Lines	0.34	87.6%
		Dist. to Sewer Overflows	0.31	
		Median Income	0.35	
Stage 2	Resilience	Resist	0.30	98.6%
		Adapt	0.51	
		Recover	0.19	

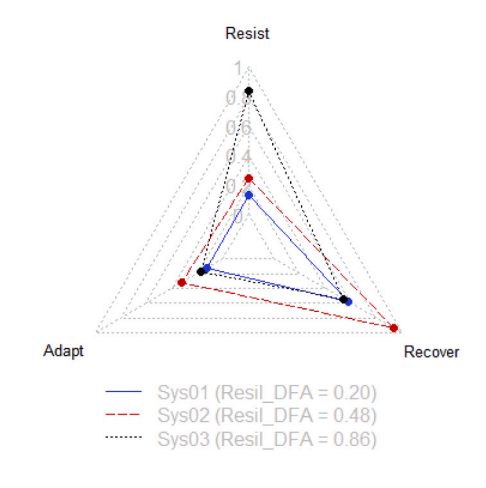
the context of the structural model, these variables are the latent constructs of their underlying latent or manifest variables. Path coefficients produced by the PLS-PM approach are presented in Table 5. These results indicate that despite their significance, the path coefficients do not seem to be entirely compatible with the premise of the proposed DFA approach, particularly the relations posited in equations (13) and (15). The results imply that impact propagation to drinking water resources has the highest path coefficient and, therefore, the highest influence in shaping the system's ability to adapt, followed by surface water and groundwater contamination according to the PLS-PM approach. However, as previously discussed in Axiom 4, impacts can't propagate to the potable water wells prior to contaminating the groundwater or freshwater resources first. Axioms of the DFA approach explicitly establish this relation resulting in high criticality in its context. In addition, all system response capacities are nearly equally important in shaping resilience, with slightly higher path coefficient values corresponding to the adaptive and recovery abilities. These findings contradict the original theory under which the resistive and adaptive capacities are expected to have a higher effect than the ability to recover, as implied by Axiom 4 and the results presented in Fig. 7.

The results of the PLS-PM indicate that although the fitness metrics obtained by this approach are statistically acceptable, the extent of the individual indicators' impact on the system response capacities and overall resilience does not entirely align with the proposed DFA approach. As expected, this gap emerges due to the differences in the formative and deductive views of the PLS-PM and DFA approaches. Before discussing the intuitions behind these observations in detail, we first examine the application of the Principal Component Analysis (PCA).

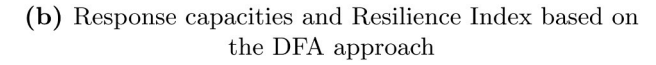
4.2. Principal component analysis (PCA)

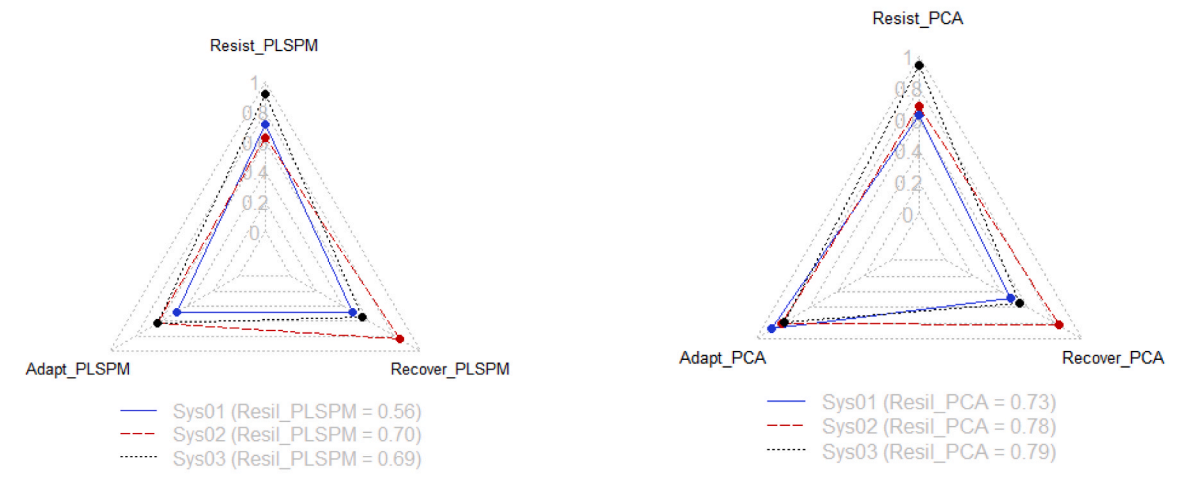
The effectiveness of PCA in mapping high-dimensional data to fewer proxies has made this approach and its extensions, such as the spatially dependent PCA (Saib et al., 2015), an appealing tool to construct composite indicators (OECD, 2008; Li et al., 2012; Kotzee and Reyers, 2016). PCA is primarily utilized to identify how different variables are associated. This is achieved by transforming the originally correlated variables into a new set of uncorrelated variables, known as Principal Components (PCs). The latter variables are calculated by combining their respective indicators using optimized weights, ensuring that the retained principal components (PCs) capture the maximum variance in the data. The evaluation of these results typically involves assessing the proportion of variance captured within the data and examining the loadings between





(a) Resilience-critical indicators for three different septic systems





- (c) Response capacities and Resilience Index based on the PLS-PM approach
- (d) Response capacities and Resilience Index based on the PCA approach

Fig. 8. Comparing Resilience Index across the DFA, PLS-PM and PCA models.

the original variables and the retained PCs.

Following the methodology adopted in constructing the Environmental Sustainability Index (Li et al., 2012, we employ a PCA-based framework for constructing the resilience composite for the OSDS case study. In this approach, similar to the DFA model, the leading indicators are grouped according to the hypothesized relations depicted in Fig. 1. The analysis is performed in two stages. In the first stage, the first set of PCs, each representing a respective system response capacity, and their factor loadings are computed. These PC scores are then used to compute the loading and the final PC score for the overall system resilience in the second stage.

The PCA results for the case study are summarized in Table 6. The results indicate that all the retained principal components representing resilience and the underlying system response capacities capture most of the variance within the data. In the first aggregation stage, we observe that indicators projecting the respective system response capacities are weighed almost equally, with a few exceptions. For the resistive capacity, the weight of distance to hydric soils, represented by the loadings, is slightly higher than the BFE and the VSD. Whereas for the adaptive capacity, the contribution of the distance to watersheds and groundwater contamination is considerably lower than other indicators. These results are not entirely aligned with the findings of the PLS-PM

and the proposed DFA approaches. While both adaptive and resistive capacities strongly influence resilience in the second stage analysis, the approaches disagree on the primary contributor to resilience. DFA emphasizes the resistive capacity, while the PCA-based approach highlights the adaptive capacity. In that respoect, the latter approach aligns more with the statistically-driven PLS-PM.

4.3. Comparative analysis

For the most part, the gaps between the DFA approach and the statistically-driven methods such as PLS-PM and PCA can be explained by the fact that the latter methods rely on correlations among variables for calculating the factor loadings and hence, the factor scores. Such reliance can be a consequential limitation since these implicitly assumed correlations do not necessarily represent the sub-indicators' actual influence on the phenomenon being assessed (Nardo et al., 2005), especially when formative relationships are considered. As such, when the indicators are aggregated to form the composite index, they fail to accurately reflect the underlying phenomenon.

We analyze and contrast how each index converts the site-related conditions into a measure of resilience using three different examples taken from the case study in order to further develop and explain this

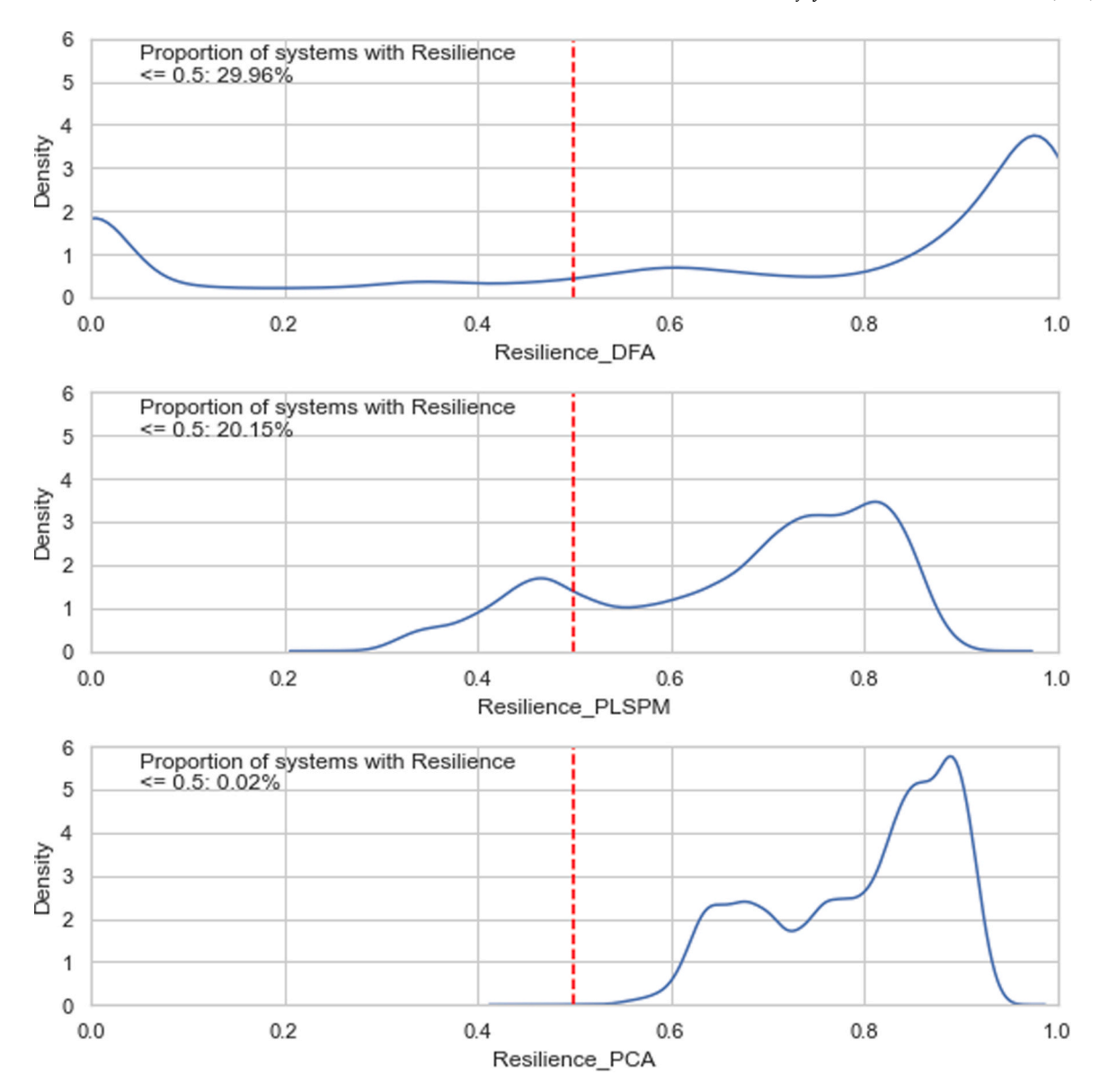


Fig. 9. Distribution of the Resilience Index computed by the proposed DFA approach, the PLS-PM, and the PCA-based model.

result. These comparisons are summarized in Fig. 8. The selected instances possess varying levels of resilience, namely, low, moderate, and high. For the system with high resilience (Sys03), the three models yield consistent resilience values with varying estimates for the system capacities. However, unlike the PLS-PM (Fig. 8c) and the PCA-based models (Fig. 8d), the proposed DFA approach results in a relatively low adaptive capacity (Fig. 8b) due to the likelihood of impact propagation to surface waters in the event of system failure. This relationship is not captured fully by the statistically-driven methods. For the system with moderate resilience (Sys02), both the resistive and adaptive capacities are low-to-moderate with high ability to recover, resulting in an overall moderate system resilience of 0.48 according to the proposed DFA model. These results do not align with the other two models, where the PLSPM and the PCA result in considerably high resilience of 0.7 and 0.78, respectively. Similarly, for the low resilience system (Sys01), the two statistically-driven models result in moderate-to-high resilience levels despite the system's low resistive, adaptive, and recovery capacities. The DFA approach, however, identifies this system's resilience to be considerably low. The differences in the obtained resilience measures can be explained by the lower weights assigned to resistivity and the linear aggregation adopted in the former approaches.

To capture the factors leading to the observed gaps in resilience measures, we generate the distributions of the resilience indices obtained by the three approaches across the entire dataset of 107,000 septic systems, as depicted in Fig. 9. It can be observed from the graph that the statistically-driven methods tend to produce moderate-to-high resilience values, with the PCA-based model yielding considerably higher values. The DFA measures, on the other hand, extend across the entire range in [0,1]. Notably, in terms of resilience, septic sites tend to cluster around low (below 0.20) and high (above 0.8) values with a nearly uniform distribution in between.

The findings highlight that the three models can yield varying levels of resilience. The approaches that rely on linear aggregation and statistically-computed weights may lead to an over-reduction of dimensionality, which can obscure the adequate representation of an indicator's importance and result in measures with "truncated domain" as illustrated in Fig. 9. In this regard, we conclude that the proposed DFA approach can be utilized to address the above-mentioned challenges and develop a composite index that; (i) aptly accounts for compensatory relations between indicators, (ii) is not prone to statistical homogeneity of data, (iii) accounts for indicators' relative importance and thus, eliminates the need for weights, and most importantly, (iv) maps the

system capacities to resilience consistently and accurately. Hence, is able to capture systems with very poor resilience (below 0.5) that need to be prioritized for adaptations.

To sum up, we reiterate that all three approaches employed in our analysis consistently agree on the significance of the selected indicators. However, they differ considerably in measuring the extent of these indicators' impact on the overall resilience of a system. While the first conclusion is relevant and essential, the second is especially critical in decision-making pertaining to resilience improvement and adaptation. Clearly, effective adaptation decisions cannot be made without correctly incorporating their impact on the objectives or criteria related to resilience. In the next section, we introduce a general framework to demonstrate how DFA-based metrics can actuate decision-making models in the context of adaptation for resilience.

5. Resilience-based decision making

While building consistent and effective metrics for resilience is a critical stage, the loop in resilience enhancement cannot be closed until these metrics are utilized to build decision models that result in effective adaptation solutions. Previous work due to Weiss et al. (2008), Molinos-Senante et al. (2012), and Abdalla et al. (2021) refer to four main strategies for adapting a septic systems to rising sea levels: (i) abandoning the existing system and connecting the site to the sewer network, (ii) considering a mound septic system by elevating the drain field, (iii) considering a non-conventional advanced treatment system, and (iv) abandoning the existing system and connecting the site to a micro (or community) sewer network with a decentralized treatment facility (also known as package plant). Each of these strategies is subject to constraints that set the limits for feasible solutions. For instance, according to the septic design and siting manual, a mound system cannot be installed if the vertical separation distance is less than 1 ft (\approx 30 cm). Also, connection to the sewer network cannot be considered when the pump station basin to which the site belongs is in moratorium condition. Moreover, financial limitations pose additional constraints when making adaptation decisions. Moreover, the decision-making framework should determine not only the "optimal" actions but also the sequence in which these actions should be implemented. This sequence can be influenced by a variety of factors, such as the resilience of the site, financial limitations, and equity.

The baseline function for resilience given in (15) can be incorporated into a decision model in several ways. It can be used to form the model's objective function, where maximization of resilience bears on the goal of the decision-making. In this context, it can also serve as one of the objectives under a multi-objective decision-making setting. Alternatively, it can be incorporated into the set of constraints to establish lower bounds on resilience under various objectives (e.g., cost minimization, equity maximization, etc.). The resilience function influences decisionmaking by responding to changes in the adaptation decision variables. For example, if the sewer extension solution is adopted, most of the resilience-critical indicators initially identified for shaping the septic system's resilience no longer constitute a threat to the functionality of the sewage collection and disposal from the site. These include distance to saturated soil, proximity to drinking water wells, and proximity to the sewer lines, given that a site is already connected. Moreover, after merging the OSTDS with the sewer system, the significance of vertical separation distance measure changes in that it now reflects the clearance between the buried components of the infrastructure, such as pipes, and the groundwater level. On the other hand, proximity to sewer overflow points may become a significant indicator as the site may coincide with a stressed section of the sewer network, making it less resistant to future stresses. Consequently, the resilience function must be updated to reflect the system's response under alternative adaptation options.

To set up the mathematical model, we let L denote the set of all possible adaptation actions, and $l \in L$ represents a particular action in this set, where l = 0 corresponds to "Do nothing." We let R_{il} denote the

resilience function for site i under adaptation action l. For example, if we let l=1 indicate the sewer line connection option, the resilience function under this option will be:

$$R_{il} = 1 - \left[\left(1 - \prod_{j=2,12} x' \right) \left(1 - \prod_{j=3,5,7,11} x' \right) \right] \quad \forall l = 1$$
 (18)

Similarly, if we let l=2 represent the option of elevating the drain field (i.e., mounding the septic system), the resilience function under this option can be rewritten as

$$R_{il} = 1 - [(1 - RC')(1 - AC_i \times SC_i)] \quad \forall l = 2$$
(19)

where, both; AC_i and SC_i follow equations (13) and (14), whereas RC' is updated using the new vertical separation distance, x_{i3}^n , expressed by:

$$x_{i3}^n = x_{i3} + y_i (20)$$

where y_i is the drain field mounding height for septic site i.

Consequently, we can develop a general adaptation decision-making framework by integrating the estimated current resilience levels and the proposed post-adaptation resilience relations. A sample framework, where resilience is incorporated as a constraint, is given by the following generic integer programming formulation:

$$Min Z \sum_{i \in N} \sum_{l \in L} c_{il} \gamma_{il} \tag{21}$$

$$\sum_{l \in I} \gamma_{il} R_{il} \ge b_i \quad \forall i \in N$$
 (22)

$$\sum_{i \in I} \gamma_{ii} = 1 \quad \forall i \in N$$
 (23)

$$\gamma_{il} \in [0,1] \quad \forall i \in N, l \in L \tag{24}$$

In this generic formulation, N is the set of septic sites, c_{il} is the cost of adopting adaptation strategy l for septic site i, and γ_{il} is the binary variable that indicates whether a strategy is selected ($\gamma_{il}=1$) or not ($\gamma_{il}=0$). The overall objective of the model is to minimize the total investment in adaptation under a constraint set that stipulates a minimum preset level of resilience for site i denoted by b_i (22). Constraint (23) ensures that exactly one adaptation strategy is selected for each site, including the do-nothing option.

The generic formulation presented here is for illustrative purposes. A more comprehensive and context-specific version would include additional operational, technological, and socio-ethical constraints, along with associated decision variables. Our aim is to demonstrate the integration of the proposed composite resilience measure into decision-making and suggest potential research directions for adaptation decision-making while explicitly considering resilience. The resilience function can be incorporated into the decision model in different ways, depending on the context. For example, it can be reconfigured to maximize resilience within budget constraints. In a broader context, the model can be customized for goal programming and multi-objective optimization, considering multiple stakeholders' perspectives. This allows the decision model to provide a range of non-dominated solutions, enabling decision-makers to evaluate alternative plans that meet various goals and stakeholder perspectives.

In real-world applications, adaptation actions are often conducted in multiple stages and periods to address budget constraints and changing environmental conditions over time, such as sea level rise projections. The proposed modeling framework can be tailored to accommodate such settings by adopting multi-stage, multi-period structures. Incorporating stochastic programming and robust optimization techniques can capture the dynamic and uncertain nature of climate change-related parameters. Integrating the proposed resilience measure into decision-making frameworks opens avenues for future research in developing large-scale mathematical programming models for regional adaptation

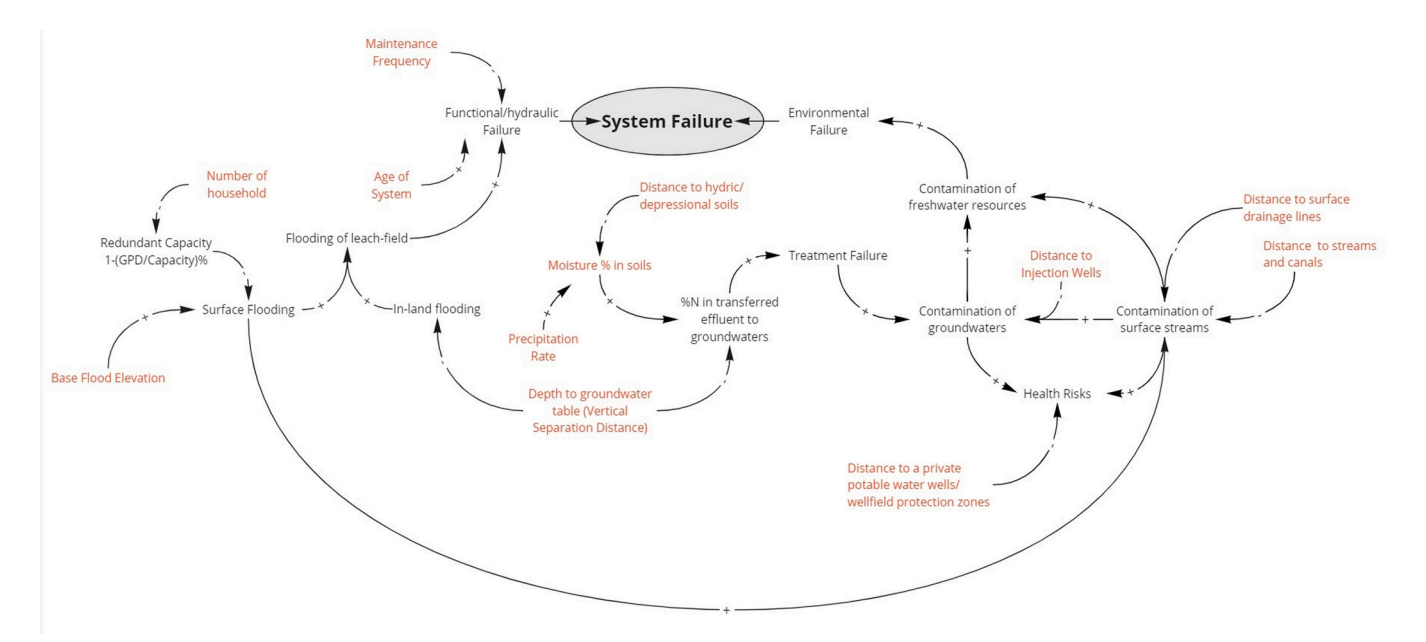


Fig. A1. CLD illustrating the mapping between OSTD system failure modes and the potential root causes.

problems. These models can address diverse objectives, constraints, and decision variables across time, space, and domain.

It is important to highlight that the DFA-based methodology proposed in this paper does not aim to completely replace traditional models such as simulations and table exercises with stakeholders. Simulation remains a valuable tool for assessing the robustness of solutions derived from index-based mathematical models and for refining the transformation functions. Additionally, the analytical structure outlined in Section 2 can be incorporated into table exercises to quantify indicators and reduce subjectivity in mapping indicators to the proposed resilience index. Thus, our proposed methodology is complementary to these approaches and can be utilized to enhance their efficacy.

6. Conclusions

Extreme stresses caused by climate change, such as the rising seas, are growing more severe, threatening different aspects of society including the infrastructure systems. To meet the gravest threats, planners and communities have been devising solutions to climate adaptation by enhancing systems' resilience. The effectiveness of the adaptation decision framework depends on how well it models resilience and incorporates it into a holistic decision-making process. Although there has been growing literature on integrating resilience into adaptation policy-making, several challenges are yet to be addressed. First, developing a multidimensional resilience index that reflects the significance of the underlying resilience-critical indicators consistently and accurately with the proper scope is challenging. Second, the failure to capture the relationship between resilience and adaptation and adequately integrate it into decision-making might lead to maladaptive outcomes.

To tackle these challenges, in this paper, we propose a framework for a composite resilience metric that can be incorporated into adaptation decision-making. In our approach, we follow the general principles of risk engineering that include hazard identification, risk analysis, risk evaluation and risk treatment. In the context of the on-site wastewater treatment and disposal systems (OSTDS), we first identify the hazards for these systems caused by the rising sea levels. We then develop a framework that employs a deductive (formative) construct based on the conditions essential for systems' survival during and after disruptions. The proposed deductive fault analysis (DFA) framework is founded on a set of axioms that map the individual resilience leading measures into a

multidimensional composite resilience index. These axioms address compensatory and non-compensatory relations between indicators. Moreover, they do not require the assumption of statistical homogeneity of data and do not resort to weights to map the system capacities to resilience. We contextualize the proposed approach using a case study based on the on-site wastewater treatment and disposal systems (OSTDS) located in Miami-Dade County in Florida.

Using the case study, we compare and contrast the proposed DFA with two statistically-driven models: the Partial-Least Squares Path Model (PLS-PM) and the Principal Component Analysis (PCA). Although all three approaches are primarily in accord with each other concerning the significance of the selected indicators, we observe that they differ considerably in measuring the extent of these indicators' impact on the overall resilience of a system. On one hand, the reliance of the statistically-driven models on the statistical homogeneity of the data and correlations among the indicators to inform weights limit their extent and spread. On the other hand, the DFA approach provides higher degrees of freedom and does not synthesize any correlations across the data set. Moreover, the latitude of incorporating compensatory relations in this approach provides an additional advantage to establishing more accurate mapping across indicators.

Although the proposed approach is demonstrated in the context of OSTDS, it can be generalized to other infrastructure systems subject to varying risks. An essential precondition is a clear understanding of the system, its various failure modes, and operating requirements. Such knowledge will help establish the premise on which the resilience-critical indicators are identified and the potential causality relations between the indicators and resilience. As a limitation, this methodology could become intricate with extensively complex systems. Under such settings, more aggregation layers may be needed to capture the complex structure, resulting in tractability challenges.

The proposed metric integrates system characteristics, environmental factors, and social factors to assess the system's resilience in resisting, adapting to, and recovering from disruptions. As a multi-dimensional measure, our resilience index can be a practical tool for decision-making, as it maps the relationships between adaptation decisions and the factors that contribute to resilience. Our transformation and modeling approaches address the challenge of incorporating resilience into quantitative and systematic decision-making processes. For future work, we intend to utilize our framework to develop comprehensive decision-making models and solution algorithms. These models

will consider a multi-period planning horizon and account for uncertainty in sea-level projections while maintaining a focus on the OSTDS.

Funding Statement

This research was partially funded by National Science Foundation (NSF), grant number 2115275.

Declaration of Competing Interest

The authors declare that they have no known competing financial interests or personal relationships that could have appeared to influence the work reported in this paper.

Appendix A. Causal Loorp Diagram (CLD) for The Exploratory Analysis

Figure A1 depicts the CLD utilized in our deductive fault analysis. The arrows in the diagram denote the direction of influence and +/- signs indicate whether the influence is upward or downward respectively. The deduced key root causes are identified and highlighted in red. These root causes serve as the basis for deriving leading indicators, which are utilized in the development of the proposed resilience index.

References

- Abdalla, H., Rahmat-Ullah, Z., Abdallah, M., Alsmadi, S., Elashwah, N., 2021. Ecoefficiency analysis of integrated grey and black water management systems. Resour., Conserv. Recycl. 172, 105681.
- Amer, L., Erkoc, M., Feagin, R.A., Kameshwar, S., Mach, K.J., Mitsova, D., 2023.
 Measuring resilience to sea-level rise for critical infrastructure systems: leveraging leading indicators. J. Mar. Sci. Eng. 11 (7), 11071421.
- Asadzadeh, A., Kötter, T., Salehi, P., Birkmann, J., 2017. Operationalizing a concept: the systematic review of composite indicator building for measuring community disaster resilience. Int. J. Disaster Risk Reduct. 25, 147–162. https://doi.org/10.1016/j. iidrr.2017.09.015.
- Azadeh, A., Salehi, V., Ashjari, B., Saberi, M., 2014. Performance evaluation of integrated resilience engineering factors by data envelopment analysis: the case of a petrochemical plant. Process Saf. Environ. Prot. 92 (3), 231–241.
- Ba-Alawi, A.H., Ifaei, P., Li, Q., Nam, K., Djeddou, M., Yoo, C., 2020. Process assessment of a full-scale wastewater treatment plant using reliability, resilience, and econosocio-environmental analyses (r2ese). Process Saf. Environ. Prot. 133, 259–274.
- Banihabib, M.E., Hashemi-Madani, F.S., Forghani, A., 2017. Comparison of compensatory and non-compensatory multi criteria decision making models in water resources strategic management. Water Resour. Manag. 31 (12), 3745–3759.
- Beccari, B., 2016. A comparative analysis of disaster risk, vulnerability and resilience composite indicators. PLoS Curr. 8. Pmid:27066298.
- Becker, J.M., Klein, K., Wetzels, M., 2012. Hierarchical latent variable models in PLS-SEM: guidelines for using reflective-formative type models. Long. Range Plan. 45 (5–6), 359–394.
- Blalock Jr, H.M., 1982. Conceptualization and measurement in the social sciences. Sage Publications, Beverly Hills, CA.
- Cataldo, R., Grassia, M.G., Lauro, N.C., Marino, M., 2017. Developments in higher-order PLS-PM for the building of a system of composite indicators. Qual. Quant. 51 (2), 657–674.
- Chen, C., Li, J., Zhao, Y., Goerlandt, F., Reniers, G., Yiliu, L., 2023. Resilience assessment and management: a review on contributions on process safety and environmental protection. Process Saf. Environ. Prot. 170, 1039–1051.
- Cutter, S.L., Barnes, L., Berry, M., Burton, C., Evans, E., Tate, E., Webb, J., 2008. A place-based model for understanding community resilience to natural disasters. Glob. Environ. Change 18 (4), 598–606.
- Demirel, H., Kompil, M., Nemry, F., 2015. A framework to analyze the vulnerability of European road networks due to sea-level rise (SLR) and sea storm surges. Transp. Res. Part A: Policy Pract. 81, 62–76.
- Gunderson, L.H., Holling, C.S., Light, S.S., 1995. Barriers and Bridges to the Renewal of Ecosystems and Institutions. Columbia University Press.
- Holling, C.S., 1973. Resilience and stability of ecological systems. Annu. Rev. Ecol. Syst. 4 (1), 1–23.
- Hollnagel, E., 2017. Epilogue: RAG the Resilience Analysis Grid. Resilience Engineering in Practice. CRC Press, pp. 275–296.
- Hollnagel, E., Woods, D.D., Leveson, N., 2006. Resilience Engineering: Concepts and Precepts. Ashgate Publishing, Ltd.
- Hosseini, S., Barker, K., Ramirez-Marquez, J.E., 2016. A review of definitions and measures of system resilience. Reliab. Eng. Syst. Saf. 145, 47–61.
- Huang, W., Ling, M., 2018. System resilience assessment method of urban lifeline system for gis. Comput., Environ. Urban Syst. 71, 67–80.
- Kline, R.B., 2015. Principles and Practice of Structural Equation Modeling. Guilford Publications.

- Knott, J.F., Jacobs, J.M., Daniel, J.S., Kirshen, P., 2019. Modeling groundwater rise caused by sea-level rise in coastal New Hampshire. J. Coast. Res. 35 (1), 143–157.
- Kotzee, I., Reyers, B., 2016. Piloting a social-ecological index for measuring flood resilience: a composite index approach. Ecol. Indic. 60, 45–53.
- Lauro, N.C., Grassia, M.G., Cataldo, R., 2018. Model based composite indicators: new developments in partial least squares-path modeling for the building of different types of composite indicators. Soc. Indic. Res. 135 (2), 421–455.
- Li, T., Zhang, H., Yuan, C., Liu, Z., Fan, C., 2012. A PCA-based method for construction of composite sustainability indicators. Int. J. Life Cycle Assess. 17 (5), 593–603.
- Lindén, D., Cinelli, M., Spada, M., Becker, W., Gasser, P., Burgherr, P., 2021.
 A framework based on statistical analysis and stakeholders' preferences to inform weighting in composite indicators. Environ. Model. Softw. 145, 105208.
- Lusk, M., Albertin, A., Elmore, W., Lester, W., Moll, J., 2020. Septic systems and springs water quality: an overview for Florida: Ss693/sl480, 10/2020. EDIS 2020 (5).
- Mengolini, A., Debarberis, L., 2008. Effectiveness evaluation methodology for safety processes to enhance organisational culture in hazardous installations. J. Hazard. Mater. 155 (1–2), 243–252.
- Molinos-Senante, M., Garrido-Baserba, M., Reif, R., Hernández-Sancho, F., Poch, M., 2012. Assessment of wastewater treatment plant design for small communities: environmental and economic aspects. Sci. Total Environ. 427, 11–18.
- Nardo, M., Saisana, M., Saltelli, A., Tarantola, S., 2005. Tools for composite indicators building. Eur. Com., Ispra 15 (1), 19–20.
- OECD, 2008. Handbook on constructing composite indicators: methodology and user guide. OECD, Paris. https://doi.org/10.1787/9789264043466-en.
- National Research Council, 2012. Disaster resilience: A national imperative. The National Academies Press, Washington, DC.
- Elmir, S. 2018. Septic systems vulnerable to sea level rise. final report in support of resolution no. Tech. rep., R-911–16.
- Global, F. 2020.FM global resilience index. Accessed on October 1 2020.
- Grabowski, M., Ayyalasomayajula, P., Merrick, J., Mccafferty, D., 2007. Accident precursors and safety nets: leading indicators of tanker operations safety. Marit. Policy Manag. 34 (5), 405–425.
- Latan, H., Noonan, R., Matthews, L. 2017. Partial least squares path modeling. Partial Least Squares Path Modeling: Basic Concepts, Methodological Issues and Applications.
- Núñez-López, J.M., Rubio-Castro, E., Ponce-Ortega, J.M., 2021. Involving resilience in optimizing the water-energy-food nexus at macroscopic level. Process Saf. Environ. Prot. 147, 259–273.
- Orencio, P.M., Fujii, M., 2013. A localized disaster-resilience index to assess coastal communities based on an analytic hierarchy process (AHP). Int. J. Disaster Risk Reduct. 3, 62–75.
- Otoiu, A., Pareto, A., Grimaccia, E., Mazziotta, M., Terzi, S., 2021. Open issues in composite indicators. A starting point and a reference on some state-of-the-art issues. vol. 3. Roma TrE-Press,.
- Panteli, M., Mancarella, P., 2015. Influence of extreme weather and climate change on the resilience of power systems: impacts and possible mitigation strategies. Electr. Power Syst. Res. 127, 259–270.
- Patriarca, R., Falegnami, A., De Nicola, A., Villani, M.L., Paltrinieri, N., 2019. Serious games for industrial safety: an approach for developing resilience early warning indicators. Saf. Sci. 118, 316–331.
- Pawar, B., Huffman, M., Khan, F., Wang, Q., 2022. Resilience assessment framework for fast response process systems. Process Saf. Environ. Prot. 163, 82–93.
- Penaloza, G.A., Saurin, T.A., Formoso, C.T., Herrera, I.A., 2020. A resilience engineering perspective of safety performance measurement systems: a systematic literature review. Saf. Sci. 130, 104864.
- Rao, C.S., Kareemulla, K., Krishnan, P., Murthy, G., Ramesh, P., Ananthan, P., Joshi, P., 2019. Agro-ecosystem based sustainability indicators for climate resilient agriculture in india: a conceptual framework. Ecol. Indic. 105, 621–633.
- Saib, M.S., Caudeville, J., Beauchamp, M., Carré, F., Ganry, O., Trugeon, A., Cicolella, A., 2015. Building spatial composite indicators to analyze environmental health inequalities on a regional scale. Environ. Health 14 (1), 1–11.
- Sanchez, G., 2013. PLS path modeling with R. Berkeley.: Trowchez Ed. 383 (2013), 551. Schneiderbauer, S., Ehrlich, D., 2006. Social levels and hazard. Meas. Vulnerability Nat. Hazard.: Towards Disaster Resilient Soc. 78.
- Shandiz, S.C., Foliente, G., Rismanchi, B., Wachtel, A., Jeffers, R.F., 2020. Resilience framework and metrics for energy master planning of communities. Energy 203, 117856.
- Sun, Y., Garrido-Baserba, M., Molinos-Senante, M., Donikian, N.A., Poch, M., Rosso, D., 2020. A composite indicator approach to assess the sustainability and resilience of wastewater management alternatives. Sci. Total Environ. 725, 138286.
- Tachaudomdach, S., Upayokin, A., Kronprasert, N., Arunotayanun, K., 2021. Quantifying road-network robustness toward flood-resilient transportation systems. Sustainability 13 (6), 3172.
- Tomaselli, V., Fordellone, M., Vichi, M., 2021. Building well-being composite indicator for micro-territorial areas through PLS-SEM and K-means approach. Soc. Indic. Res. 153 (2), 407–429.
- Tong, Q., Gernay, T., 2023. Resilience assessment of process industry facilities using dynamic bayesian networks. Process Saf. Environ. Prot. 169, 547–563.
- Vajjarapu, H., Verma, A., 2021. Composite adaptability index to evaluate climate change adaptation policies for urban transport. Int. J. Disaster Risk Reduct. 58, 102205.
- Weiss, P., Eveborn, D., Kärrman, E., Gustafsson, J.P., 2008. Environmental systems analysis of four on-site wastewater treatment options. Resour., Conserv. Recycl. 52 (10), 1153–1161.
- Yarveisy, R., Gao, C., Khan, F., 2020. A simple yet robust resilience assessment metrics. Reliab. Eng. Syst. Saf. 197, 106810.